HHS Public Access

Author manuscript

Cell Rep. Author manuscript; available in PMC 2019 August 06.

Published in final edited form as:

Cell Rep. 2019 July 23; 28(4): 1050–1062.e6. doi:10.1016/j.celrep.2019.06.078.

Translational Regulation of Non-autonomous Mitochondrial Stress Response Promotes Longevity

Jianfeng Lan[1,4], **Jarod A. Rollins**[2,4], **Xiao Zang**[1,4], **Di Wu**[1,4], **Lina Zou**[1], **Zi Wang**[1], **Chang Ye**[1], **Zixing Wu**[1], **Pankaj Kapahi**[3,*], **Aric N. Rogers**[2,*], **Di Chen**[1,5,*]

[1]State Key Laboratory of Pharmaceutical Biotechnology and MOE Key Laboratory of Model Animals for Disease Study, Model Animal Research Center, Institute for Brain Sciences, Nanjing University, 12 Xuefu Rd, Pukou, Nanjing, Jiangsu 210061, China

[2]MDI Biological Laboratory, 159 Old Bar Harbor Rd., Salisbury Cove, ME 04672, USA

[3]Buck Institute for Research on Aging, 8001 Redwood Boulevard, Novato, CA 94945, USA

[4]These authors contributed equally

[5]Lead Contact

SUMMARY

Reduced mRNA translation delays aging, but the underlying mechanisms remain underexplored. Mutations in both DAF-2 (IGF-1 receptor) and RSKS-1 (ribosomal S6 kinase/S6K) cause synergistic lifespan extension in *C. elegans*. To understand the roles of translational regulation in this process, we performed polysomal profiling and identified translationally regulated ribosomal and cytochrome *c* (CYC-2.1) genes as key mediators of longevity. *cyc-2.1* knockdown significantly extends lifespan by activating the intestinal mitochondrial unfolded protein response (UPR^{mt}), mitochondrial fission, and AMP-activated kinase (AMPK). The germline serves as the key tissue for *cyc-2.1* to regulate lifespan, and germline-specific *cyc-2.1* knockdown non-autonomously activates intestinal UPR^{mt} and AMPK. Furthermore, the RNA-binding protein GLD-1-mediated translational repression of *cyc-2.1* in the germline is important for the non-autonomous activation of UPR^{mt} and synergistic longevity of the *daf-2 rsks-1* mutant. Altogether, these results illustrate a translationally regulated non-autonomous mitochondrial stress response mechanism in the modulation of lifespan by insulin-like signaling and S6K.

Graphical Abstract

*Correspondence: pkapahi@buckinstitute.org (P.K.), arogers@mdibl.org (A.N.R.), chendi@nju.edu.cn (D.C.).

AUTHOR CONTRIBUTIONS

J.L., X.Z., and D.W. performed experiments. J.A.R. performed experiments and bioinformatics analysis. L.Z., Z. Wang, C.Y., and Z. Wu provided technical assistance. D.C., A.N.R., and P.K. conceived the project, designed experiments, and wrote the paper.

SUPPLEMENTAL INFORMATION

Supplemental Information can be found online at https://doi.org/10.1016/j.celrep.2019.06.078.

DECLARATION OF INTERESTS

The authors declare no competing interests.

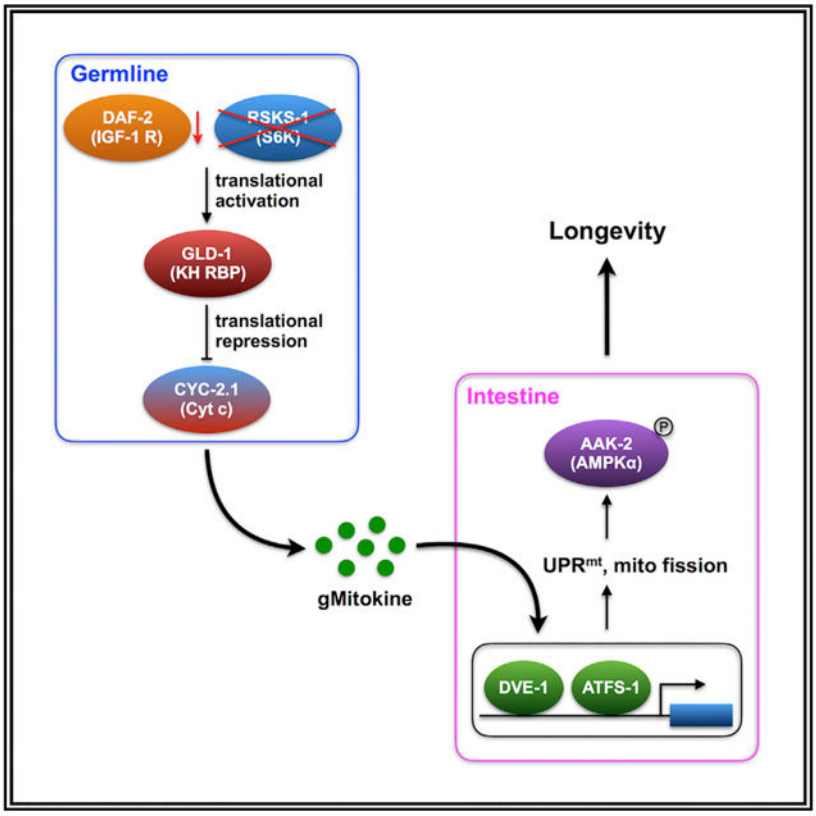

In Brief

To understand how reduced translation delays aging, Lan et al. perform translational profiling in *C. elegans* and propose that, in the significantly long-lived *daf-2 rsks-1* mutant, serial translational regulation leads to reduced cytochrome *c* in the germline, which non-autonomously activates UPR^{mt} and AMPK in the metabolic tissue to ensure longevity.

INTRODUCTION

Aging can be genetically modulated by perturbation of insulin/insulin-like signaling (IIS), target of rapamycin (TOR) pathway, and mitochondrial functions (Fontana et al., 2010; Kenyon, 2010; López-Otín et al., 2013). These genetic manipulations often lead to significant changes in gene expression at both transcriptional and translational levels. Inhibition of DAF-2, the *C. elegans* ortholog of the insulin growth factor 1 (IGF-1) receptor, doubles adult lifespan by activating the DAF-16 (FOXO) transcriptional factor to regulate downstream genes involved in stress resistance, detoxification, and metabolism (Kenyon et al., 1993; Kimura et al., 1997; Lin et al., 1997; McElwee et al., 2004; Murphy et al., 2003; Ogg et al., 1997). Quantitative proteomics and polysomal profiling studies revealed that the *daf-2* mutant also shows altered mRNA translation in many genes, and translational regulation plays important roles in significantly prolonged longevity and extended survival during heat stress (Depuydt et al., 2013; Dong et al., 2007; McColl et al., 2010; Stout et al., 2013).

Inhibition of the TOR pathway significantly extends lifespan in many species (Kapahi et al., 2010). One important function of TOR is to regulate gene expression at the mRNA translation level through the ribosomal S6 kinase (S6K) and the translational initiation factor 4E-binding protein (4E-BP), both of which have been shown to play important roles in aging (Hansen et al., 2007; Kapahi et al., 2004; Pan et al., 2007; Zid et al., 2009). Deletion mutants of *rsks-1*, which encodes the *C. elegans* ribosomal S6K ortholog, lead to significant changes in development, lipid metabolism, reproduction, and longevity (Hansen et al., 2007; Korta et al., 2012; Pan et al., 2007; Shi et al., 2013). Previous studies have identified multiple mediators of the prolonged longevity of the *rsks-1* mutant (Chen et al., 2009; McQuary et al., 2016; Selman et al., 2009; Seo et al., 2013; Sheaffer et al., 2008). However, genes translationally regulated by RSKS-1 that influence lifespan and the underlying molecular mechanisms remain to be characterized.

Serving as the key organelle in energy homeostasis, mitochondria play important but complex roles in aging. Mitochondrial dysregulation has been regarded as one of the major hallmarks of aging. However, mild perturbation of the mitochondrial electron transport chain (ETC) leads to significant lifespan extension in many species (Dillin et al., 2002; Houtkooper et al., 2013; Lee et al., 2003; López-Otín et al., 2013). Inhibition of mitochondrial ETC genes triggers the mitochondrial unfolded protein response (UPR^{mt}) via transcriptional regulators such as DVE-1, UBL-5, and ATFS-1 (Haynes et al., 2007; Nargund et al., 2012). Perturbation of mitochondrial ETC functions in neurons releases a pro-longevity cue named mitokine to induce UPR^{mt} in the intestine, a distal metabolic tissue in worms, and ensures lifespan extension (Durieux et al., 2011). Further studies have identified the neurotransmitter serotonin, neuropeptide FLP-2, and retromer-dependent Wnt signaling as the endocrine mediators of the neuron to intestine non-autonomous mitochondrial stress response (Berendzen et al., 2016; Shao et al., 2016; Zhang et al., 2018). The trans-tissue mitochondrial stress response requires epigenetic modifications that ensure selective gene expression and prolonged longevity, and the epigenetic regulatory mechanisms are conserved in mammals (Merkwirth et al., 2016; Tian et al., 2016).

To study how insulin-like signaling interacts with the TOR pathway to modulate aging, we previously constructed a *daf-2 rsks-1* double mutant and observed a synergistic longevity phenotype. Further analysis demonstrated an AMP-activated kinase (AMPK)-mediated positive feedback regulation of the DAF-16 transcriptional factor mechanism in the *daf-2 rsks-1* mutant (Chen et al., 2013). However, genes that are translationally regulated in the *daf-2 rsks-1* mutant and their roles in aging have not been determined. Because both *daf-2* and *rsks-1* have profound impacts on mRNA translation, we hypothesized that translational regulation plays important roles in the significantly prolonged longevity of *daf-2 rsks-1* mutant animals. By genome-wide translational state analysis and genetic screens, we identified ribosomal protein genes and *cyc-2.1*, which encodes one of the worm cytochrome *c* orthologs, as negative regulators of longevity. The inhibition of *cyc-2.1* results in a robust lifespan extension that requires UPR^{mt}, AMPK, and mitochondrial fission in the intestine. Germline is the key tissue for *cyc-2.1* to regulate longevity, and inhibition of *cyc-2.1* in the germline initiates a cell non-autonomous response that activates UPR^{mt} and AMPK in the intestine. Based on the translational profiling, we identified the RNA-binding protein GLD-1 as a critical translational repressor of *cyc-2.1* in the germline. The synergistic lifespan

extension of the *daf-2 rsks-1* mutant can be suppressed by inhibiting GLD-1 or key transcriptional regulators of UPR^{mt}. Therefore, the insulin-like signaling and TOR pathway-mediated tissue-specific translational repression of cytochrome *c* induce a cell non-autonomous mitochondrial stress response to promote longevity.

RESULTS

Genome-wide Translational State Analysis of the Significantly Long-Lived *daf-2 rsks-1* Mutant

To characterize the roles of mRNA translation in the significantly prolonged longevity of *daf-2 rsks-1*, we performed genome-wide translational state analysis via polysomal profiling coupled with RNA sequencing (RNA-seq) using wild-type N2 and *daf-2 rsks-1* mutant animals (Figure 1A). Day 4 adult animals were collected for extraction of total mRNAs and translated mRNAs (≥2 ribosomes/transcript) for quantification via RNA-seq (Figure 1A). Gene set enrichment analysis (GSEA) was performed to compare RNA-seq results with our previous microarray studies (Chen et al., 2013). Transcriptionally up- and downregulated gene lists both showed significant concordance with the microarray results (false discovery rate [FDR] < 0.001), with normalized enrichment scores of 2.84 and 3.19, respectively (Figure S1). Changes in translation were determined by comparing the ratio of polysome-associated mRNAs to total mRNAs between N2 and *daf-2 rsks-1* mutant animals. This is called the differential polysome association ratio (DPAR). Altogether, we identified 167 transcripts with differential translation but no changes at total mRNA levels. Among them, 52 genes are upregulated and 115 genes are downregulated in the *daf-2 rsks-1* mutant (Figure 1B; Table S1). Gene Ontology (GO) enrichment analysis of biological processes revealed meiotic cell cycle, cell cycle, and organelle fission are the top three terms in the upregulated genes, whereas translation, ribosome biogenesis, and developmental process are the top three terms in the downregulated genes (Figure 1C).

To validate whether mRNAs with differential ribosome loading are regulated at the mRNA translational level, we compared expression of *rps-0*, *rps-3*, *rpl-5*, and *rpl-25.2* at both mRNA and protein levels between N2 and *daf-2 rsks-1* mutant animals. These genes were chosen based on the availability of antibodies (Liu et al., 2018) to detect their protein products. Consistent with the RNA-seq data (Table S1), mRNA levels of *rps-0*, *rps-3*, *rpl-5*, and *rpl-25.2* show no significant changes between N2 and *daf-2 rsks-1* mutant animals (Figure 1D), whereas protein products of these genes are significantly decreased in the *daf-2 rsks-1* mutant compared with N2 (Figures 1E and 1F). Previous quantitative proteomics studies also showed that the abundance of these ribosomal proteins is decreased in the *daf-2* mutant compared with N2 (Depuydt et al., 2013; Stout et al., 2013). Altogether, these results indicate that polysomal profiling is a valid approach to quantitatively assess mRNA translation, which allowed us to identify differentially translated mRNAs in the *daf-2 rsks-1* mutant.

Genes Downregulated in the *daf-2 rsks-1* Mutant Are Enriched with Lifespan Determinants

Numerous studies have demonstrated that genes differentially expressed in long-lived mutants are key regulators of lifespan. We thus hypothesized that genes translationally

downregulated in the long-lived *daf-2 rsks-1* mutant are likely to be negative regulators of longevity, inhibition of which in the wild-type background could extend lifespan. Thus, we performed an RNAi-based genetic screen to individually knockdown those 115 translationally downregulated genes in N2 to test their effects on lifespan. To facilitate the survival assays, the primary screen was performed at 25°C using the *spe-9*; *rrf-3* double mutant, which shows enhanced RNAi sensitivity, temperature-sensitive sterility, and normal lifespan. Intriguingly, 39 of the 115 RNAi treatments during development led to larval arrest, suggesting that genes translationally downregulated in the *daf-2 rsks-1* mutant are enriched with developmentally essential genes. We then performed RNAi treatments against these 39 genes only during adulthood to test their lifespan phenotypes. After the re-test in the wild-type background at 20°C, we identified 24 genes, inhibition of which leads to significant lifespan extension (Table S2). Among them, 17 genes are essential ones that encode various ribosomal subunits. These results highlight the importance of developmentally essential genes and translationally regulated ribosomal biogenesis in lifespan determination.

Inhibition of CYC-2.1 Results in Robust Lifespan Extension that Requires UPR^{mt} and AMPK

Among all genes tested, *cyc-2.1*, which encodes one of the two highly conserved cytochrome *c* orthologs, showed the strongest lifespan extension upon RNAi knockdown (Table S2). *cyc-2.1* was originally identified as a lifespan determinant from an RNAi screen for enhanced oxidative stress resistance (Kim and Sun, 2007). Knockdown of *cyc-2.1* robustly extends lifespan in the wild-type, *rsks-1* mutant, and *daf-2* mutant backgrounds, but it does not further extend lifespan of the *daf-2 rsks-1* double mutant (Figure 2A; Table S3). These results suggest that reduced CYC-2.1 might serve as the key mechanism in mediating the synergistic effect of *daf-2 rsks-1* on longevity.

Cytochrome *c* functions in the mitochondrial ETC by transferring electrons from complex III to complex IV. Previous studies demonstrated that inhibition of certain mitochondrial ETC components extends lifespan, and the underlying mechanisms involve CEP-1/p53 (Baruah et al., 2014), the intrinsic apoptosis pathway (Yee et al., 2014), and UPR^{mt} (Dillin et al., 2002; Durieux et al., 2011; Lee et al., 2003). Mutations in the *C. elegans* p53 ortholog CEP-1 or a key component of the apoptosis pathway CED-4 significantly suppress the lifespan extension by mitochondrial ETC mutants (Baruah et al., 2014; Yee et al., 2014). However, *cyc-2.1* RNAi treatment significantly extends lifespan in *cep-1* or *ced-4* knockout mutant (Figures S2A and S2B), suggesting a different mechanism.

To examine the effect of *cyc-2.1* knockdown on the mitochondrial stress response, we applied *cyc-2.1* RNAi to transgenic animals carrying a *gfp* reporter driven by the *hsp-6* promoter, which has been widely used to monitor UPR^{mt} activation. Inhibition of *cyc-2.1* significantly activates *hsp-6p::gfp* reporter expression (Figure 2B). Because the *hsp-6p::gfp* reporter is mainly expressed in the intestine, we performed micro-dissection to isolate the intestinal tissue of wild-type animals treated with the control or *cyc-2.1* RNAi for qRT-PCR of the endogenous *hsp-6* mRNA. Consistent with the *hsp-6p::gfp* reporter results, knockdown of *cyc-2.1* significantly increases *hsp-6* mRNA levels compared with the control RNAi treatment (Figure 2C). Previous studies have identified ATFS-1 as one of the key

transcription factors that mediate the UPR^{mt} activation (Nargund et al., 2012). The *cyc-2.1* RNAi-induced longevity phenotype is suppressed by a deletion mutant of *atfs-1* (Figure 2D; Table S3). Therefore, activated mitochondrial stress response plays an essential role in cytochrome *c* knockdown-induced lifespan extension.

It has been reported that paraquat, a ROS (reactive oxygen species) generator, and hypomorphic mutations in mitochondrial ETC genes, such as *isp-1*, extend *C. elegans* lifespan by activating AMPK (Hwang et al., 2014). The synergistic lifespan extension by *daf-2 rsks-1* also requires AMPK (Chen et al., 2013). We performed immunoblots to measure the levels of phosphorylated AAK-2 (AMPKα), which serve as an indicator of AMPK activation, in control or *cyc-2.1* RNAi-treated animals. Knockdown of *cyc-2.1* significantly increases phospho-AAK-2 levels compared with the control (Figures 2E and 2F). Consistently, *cyc-2.1* RNAi fails to extend lifespan of the *aak-2* deletion mutant (Figure 2G; Table S3). Therefore, inhibition of *cyc-2.1* activates UPR^{mt} and AMPK to extend lifespan.

AMPK Functions Downstream of UPR^{mt} upon *cyc-2.1* Knockdown

To characterize the relationship between UPR^{mt} and AMPK in animals treated with *cyc-2.1* RNAi, we first measured phospho-AAK-2 levels in the *atfs-1* deletion mutant treated with either control or *cyc-2.1* RNAi. Immunoblots and quantification results indicate that unlike in the N2 background (Figures 2E and 2F), *cyc-2.1* RNAi does not increase phospho-AAK-2 levels in the *atfs-1* mutant (Figures 2H and 2I). We then crossed the *hsp-6* promoter::*gfp* reporter into the *aak-2* deletion mutant. In the absence of AAK-2, *cyc-2.1* RNAi still significantly activates the *hsp-6::gfp* reporter (Figure 2J), as well as the endogenous *hsp-6* transcription in the intestine (Figure 2K). Altogether, these results demonstrate that AMPK functions downstream of UPR^{mt} activation to promote lifespan extension produced by the *cyc-2.1* RNAi treatment.

cyc-2.1 Functions in the Germline to Regulate Lifespan

To determine the key tissue in which *cyc-2.1* functions to regulate lifespan, we performed tissue-specific RNAi experiments to knockdown *cyc-2.1* in the germline, intestine, epidermis, and muscles. Spatially restricted RNAi knockdown was achieved by tissue-specific promoters driving transgene rescue of mutations in *rde-1*, which is essential for the RNAi machinery to be functional (Espelt et al., 2005; Qadota et al., 2007; Zou et al., 2019). Knockdown of *cyc-2.1* in the germline significantly extends lifespan (Figure 3A; Figure S3A; Table S3), whereas knockdown of *cyc-2.1* in the intestine, epidermis, or muscles does not extend lifespan (Figure 3A; Figures S3B-S3D; Table S3). The importance of germline in *cyc-2.1* RNAi-induced lifespan extension is supported by evidence that knockdown of *cyc-2.1* in the germline-less *glp-4(ts)* mutant (Beanan and Strome, 1992) only results in mild lifespan extension by 9% (Figure S3E). Altogether, these results demonstrate that germline is the key tissue in which CYC-2.1 functions to regulate lifespan.

Germline Knockdown of *cyc-2.1* Non-autonomously Activates UPR^{mt} and AMPK in the Intestine to Extend Lifespan

To better understand whether *cyc-2.1* RNAi activates UPR^{mt} in a tissue-specific manner, we performed qRT-PCR experiments to measure mRNA levels of several ATFS-1 direct target genes, including *hsp-6*, *dnj-10*, *timm-17*, and *drp-1*, transcription levels of which are elevated upon mitochondrial ETC perturbation (Nargund et al., 2012, 2015). Gonadal and intestinal tissues were dissected from wild-type animals treated with either control or *cyc-2.1* RNAi for qRT-PCR assays. Because the gonad is 95% germline and 5% somatic gonad, and the germline and somatic gonad cannot be further dissected, we used the gonadal tissue as a proxy for the germline in subsequent experiments. Surprisingly, global *cyc-2.1* RNAi treatment significantly activates UPR^{mt} markers in the intestine, but not in the germline (Figure 3B), although the latter is the tissue in which *cyc-2.1* functions to regulate lifespan. Consistently, global *cyc-2.1* RNAi treatment significantly activates AMPK in the intestine, but not in the gonad (Figures 3C and 3D). The *aak-2* deletion mutant carrying a single-copy *aak-2* transgene driven by the *vha-6* intestine-specific promoter shows a 45% lifespan extension upon *cyc-2.1* RNAi treatment (Figure 3E; Table S3). The intestinal AAK-2 is therefore sufficient to extend lifespan substantially upon *cyc-2.1* RNAi knockdown.

Germline *cyc-2.1* Knockdown Induces Intestinal UPR^{mt} and AMPK Activation and Lifespan Extension

We next tested whether tissue-specific knockdown of *cyc-2.1* could activate UPR^{mt}and AMPK. Although both germline and intestinal-specific *cyc-2.1* RNAi treatments significantly activate UPR^{mt} markers in the intestine (Figure 3F), only germline, not intestinal, *cyc-2.1* RNAi treatment leads to increased phospho-AAK-2 levels in the intestine (Figures 3G and 3H). Because there is no direct physical contact between gonad and intestine, these results suggest the existence of endocrine-like signaling for cell non-autonomous regulation.

C. elegans has six macrophage-like coelomocytes that take up soluble macromolecules in the body cavity via endocytosis. Coelomocytes have direct physical contact with the gonad and intestine. CUP-4, an ion channel, is required for endocytosis in coelomocytes (Patton et al., 2005). When treated with the germ-line-specific *cyc-2.1* RNAi, the *cup-4* mutant cannot activate UPR^{mt} (Figure 3I) and AMPK (Figures 3J and 3K) in the intestine or extend lifespan (Figure 3L; Table S3). Altogether, these results indicate the existence of gonad to intestine signaling that regulates UPR^{mt}, AMPK, and lifespan in response to cytochrome *c* reduction in the germline.

DRP-1-Mediated Mitochondrial Fission Plays an Important Role in *cyc-2.1* Knockdown-Induced AMPK Activation and Lifespan Extension

RNAi knockdown of *cyc-2.1* leads to the transcriptional upregulation of several ATFS-1 targets, including *drp-1*, which encodes a dynamin-related protein that is required for mitochondrial fission (Breckenridge et al., 2008). Using a transgenic line that expresses the TOMM-20 mitochondria outer membrane protein fused with the mKate2 fluorescent protein in the intestine (Ahier et al., 2018), we found that knockdown of *cyc-2.1* significantly

increases intestinal mitochondrial fragmentation (Figures 4A and 4B). Blocking the mitochondrial fission by a *drp-1* knockout mutant significantly suppresses *cyc-2.1* knockdown-induced AMPK activation (Figures 4C and 4D). *cyc-2.1* RNAi treatment extends lifespan in wild-type animals by 66%, whereas the mean lifespan extension is significantly decreased to 42% in the *drp-1* mutant (Figures 4E and 3F; Table S3). Therefore, DRP-1-mediated changes in mitochondrial dynamics serve as the key mechanism for cytochrome *c* reduction-induced lifespan extension.

Tissue-Specific Activation of UPR^{mt} Contributes to the Significantly Prolonged Longevity of the *daf-2 rsks-1* Mutant

cyc-2.1 was identified as one of the genes that show significantly decreased ribosomal loading in the *daf-2 rsks-1* mutant compared with the wild-type N2 from the translational profiling analysis (Table S1). To examine whether CYC-2.1 is repressed at the protein level in the *daf-2 rsks-1* mutant, we used a CRISPR/Cas9-based genome editing approach to knock in a 3x FLAG tag to the C terminus of CYC-2.1 for immunoblots using anti-FLAG antibodies. CYC-2.1 protein levels are significantly reduced in the gonad, but not in the intestine, of the *daf-2 rsks-1* mutant (Figures 5A and 5B). qRT-PCR measurement of UPR^{mt} markers using dissected tissues demonstrates that the *daf-2 rsks-1* mutant has UPR^{mt} activation in the intestine, but not in the gonad (Figure 5C).

Previous studies showed that transcriptional factors DVE-1 and ATFS-1, as well as UBL-5, a small ubiquitin-like factor that serves as the co-factor for DVE-1, are the key mediators of UPR^{mt} (Haynes et al., 2007; Nargund et al., 2012). Inhibition of *dve-1* by RNAi shortens N2 lifespan, whereas *ubl-5* or *atfs-1* RNAi treatment does not affect N2 lifespan (Figure 5D; Table S3). The prolonged longevity of *daf-2 rsks-1* mutant animals can be significantly decreased by *dve-1, ubl-5*, or *atfs-1* RNAi (Figure 5E; Table S3). Knockdown of these key transcriptional regulators of UPR^{mt} significantly decreases the lifespan extension produced by the *daf-2 rsks-1* double mutant (Figure 5F). Therefore, the *daf-2 rsks-1* mutant shows germline reduction of CYC-2.1 and intestinal activation of UPR^{mt}, which is required for significantly prolonged longevity.

GLD-1-Mediated Translational Repression of CYC-2.1 Is Important for the UPR^{mt} Activation and Significantly Prolonged Longevity of the *daf-2 rsks-1* Mutant

Specific translational regulations in many cases are mediated by RNA-binding proteins and their association with 5′ UTRs or 3′ UTRs . GLD-1, a K homology (KH) RNA-binding protein, is regulated by GLP-1/Notch signaling to negatively regulate target genes' translation in the germline (Kimble and Crittenden, 2005). Our previous studies showed that a *glp-1* gain-of-function mutation, which decreases GLD-1 expression, suppresses the significantly extended lifespan of *daf-2 rsks-1* (Chen et al., 2013). The genome-wide translational state analysis indicates that *gld-1* mRNAs have elevated ribosomal loading in the *daf-2 rsks-1* mutant (Table S1). These results suggest that the germline-specific translational repressor GLD-1 might be involved in regulating CYC-2.1 protein levels in the germline of the *daf-2 rsks-1* mutant.

To test whether GLD-1 is upregulated in the *daf-2 rsks-1* mutant, we first performed CRISPR/Cas9-based genome editing experiments to knock in the mKate2 red fluorescent protein coding sequence to the 3′ of *gld-1*. Compared with the wild-type control, GLD-1::mKate2 protein levels are significantly increased in the germline of *daf-2 rsks-1* mutant animals (Figures 6A and 6B). To examine whether GLD-1 is involved in the translational regulation of *cyc-2.1*, we applied *gld-1* RNAi to the *daf-2 rsks-1* mutant and found that CYC-2.1 protein levels are significantly elevated in the gonad, but not in the intestine, when compared with the control RNAi-treated animals (Figures 6C and 6D). Consistently, RNAi knockdown of *gld-1* significantly decreases UPR^{mt} in the intestine of *daf-2 rsks-1* mutant animals (Figure 6E). Although *gld-1* RNAi treatment has little effect on lifespan in the wild-type and *daf-2* mutant backgrounds, knockdown of *gld-1* significantly decreases lifespan of the *rsks-1* mutant and *daf-2 rsks-1* double mutant (Figure 6F; Table S3). Altogether, these results demonstrate that GLD-1 functions as a translational repressor of *cyc-2.1* in the germline to non-autonomously activate intestinal UPR^{mt} and extend lifespan in the *daf-2 rsks-1* mutant.

In summary, we have performed genome-wide translational state analysis via polysomal profiling coupled with RNA-seq and identified genes that are regulated at the translational level in the significantly long-lived *daf-2 rsks-1* mutant. Mechanistically, we demonstrated that the GLD-1 RNA-binding protein is upregulated at the protein level in the germline of *daf-2 rsks-1* mutant. Elevated GLD-1 leads to translational repression of CYC-2.1 in the germline, which non-autonomously activates UPR^{mt} and AMPK in the intestine and significantly extends lifespan (Figure 6G). These results highlight the importance of translational regulation of a highly conserved mitochondrial gene in the significantly prolonged longevity exerted by inhibiting both insulin-like signaling and S6K.

DISCUSSION

Highly conserved IIS and the TOR pathway play an important role in aging across species (Fontana et al., 2010; Kenyon, 2010). To examine how these pathways interact with each other to modulate aging, we previously constructed a *daf-2 rsks-1* double mutant that carries loss-of-function mutations in the DAF-2/IGF-1 receptor and TOR effector RSKS-1/S6K. The double mutant shows a synergistic effect, rather than an additive effect, on longevity, suggesting active interactions between these two important aging-related pathways. Functional genomics studies via transcriptome profiling helped to identify AMPK-mediated positive feedback regulation of the DAF-16/ FOXO transcription factor mechanism in the *daf-2 rsks-1* mutant (Chen et al., 2013). However, RSKS-1, which serves as a key regulator of mRNA translation, has not been well characterized for its roles in the significantly extended longevity of *daf-2 rsks-1* mutant animals.

It has been well documented that inhibition of translation delays aging (Hansen et al., 2007; Kapahi et al., 2004, 2010; Pan et al., 2007; Rogers et al., 2011). One hypothesis is that reduced global translation helps organisms to maintain better protein homeostasis, dysregulation of which leads to aging and age-related pathologies. A linked hypothesis suggests that the anti-aging effect is achieved by the translational regulation of key modulators of aging. We reasoned that identification of genes that are translationally

regulated in the *daf-2 rsks-1* mutant and characterization of the translational regulation should help in gaining better mechanistic insights into the significantly extended longevity of the *daf-2 rsks-1* double mutant.

Through genome-wide translational state analysis and genetic screens, we identified 24 negative regulators of longevity from the 115 genes that are translationally downregulated in the *daf-2 rsks-1* mutant. One observation was that the lifespan determinants are enriched with developmentally essential genes (71%). Inhibition of these genes during development causes larval arrest, whereas RNAi knockdown only during adulthood leads to significant lifespan extension (Table S2). These results support the antagonistic pleiotropy theory of aging, which proposes that aging is adaptive, because natural selection favors genes that confer benefits during development but cause deleterious effects later in life (Williams, 1957). Thus, inhibition of developmentally essential genes during adulthood might extend lifespan (Chen et al., 2007; Curran and Ruvkun, 2007). All developmentally essential, lifespan-determinant genes encode various ribosomal subunits (Table S2), which is consistent with previous studies showing that TOR-mediated ribosomal biogenesis plays an important role in aging (Steffen et al., 2008). In addition, 13 of the 17 identified ribosomal genes showed decreased protein levels in the *daf-2* mutant or in nutrients restricted animals from previous quantitative proteomics studies (Depuydt et al., 2013; Stout et al., 2013), which highlights the important role of reduced mRNA translation in the delay of aging.

Among the lifespan regulators that we identified, knockdown of *cyc-2.1*, which encodes a highly conserved cytochrome *c* ortholog that functions in the mitochondrial ETC, results in the most significant lifespan extension (Table S2; Figure 2A). Inhibition of genes encoding components of mitochondrial respiratory complexes extends lifespan (Dillin et al., 2002; Houtkooperet al., 2013; Lee et al., 2003), and the underlying mechanisms involve UPR^{mt} (Durieux et al., 2011), CEP-1/p53 (Baruah et al., 2014), and the intrinsic apoptosis pathway (Yee et al., 2014). CEP-1 and CED-4 from the intrinsic apoptosis pathway are not required for *cyc-2.1* RNAi-induced lifespan extension (Figures S2A and S2B). Inhibition of *cco-1*, which encodes the cytochrome *c* oxidase-1 subunit Vb/COX4, significantly extends lifespan (Dillin et al., 2002). ATFS-1 is partially required for *cco-1* RNAi-induced lifespan extension (Figure S2C), whereas prolonged longevity by *cyc-2.1* RNAi can be suppressed by an *atfs-1* deletion mutant (Figure 2D; Table S3). Unlike *cyc-2.1*, intestine-specific knockdown of *cco-1* is sufficient to significantly extend lifespan (Figure S2D). Altogether, these results suggest that *cyc-2.1* might function through different mechanisms to regulate lifespan.

Previous studies showed that perturbation of mitochondrial ETC in *C.* elegans neurons provokes a pro-longevity signal to non-autonomously activate UPR^{mt} in the intestine (Berendzen et al., 2016; Durieux et al., 2011; Shao et al., 2016). In this study, we found that inhibition of *cyc-2.1* in the germline non-autonomously activates UPR^{mt} and AMPK in the intestine. Although intestine-specific *cyc-2.1* RNAi also activates UPR^{mt}, it fails to activate AMPK and extend lifespan (Figures 3A and 3F-3H; Figure S3B; Table S3). These results indicate that activation of UPR^{mt} is required, but not sufficient, for the lifespan extension produced by *cyc-2.1* knockdown. Because there is no direct contact between the germline and the intestine in *C. elegans*, we propose that reduced cytochrome *c* in the germline might produce an endocrine-like signaling, named gMitokine (germline-produced mitokine), to

activate UPR^{mt} in the distal tissue for prolonged survival. The germline to intestine regulation can be blocked by the *cup-4* mutant, which disrupts endocytosis in coelomocytes (Figures 3I-3L). Altogether, our findings demonstrate a cell non-autonomous signaling that is distinctive from the neuron to intestine mitokine pathways. Further characterization of this germline to intestine signal transduction process, especially identifying the gMitokine and its downstream effectors, will help in better understanding UPR^{mt}-mediated anti-aging mechanisms.

The germline tissue plays an important role in *C. elegans* aging. Germline-less worms showed significant lifespan extension that depends on the DAF-16 FOXO transcription factor and DAF-12 nuclear hormone receptor. The prolonged longevity of germline-less animals is not due to sterility; rather, it is caused by diminished pro-aging signaling from the germline (Berman and Kenyon, 2006; Hsin and Kenyon, 1999). However, the molecular identity of aging signals produced by germ cells has not been fully determined. We speculate that *cyc-2.1* knockdown and germline deficiency function through different mechanisms to regulate lifespan, because unlike the long-lived germline-less animals, the *cyc-2.1* RNAi-treated animals show significantly prolonged longevity independent of DAF-16 or DAF-12 (Figure S3F).

It has been shown that the germline is the key tissue for RSKS-1 to regulate lifespan. Knockdown of *rsks-1* in the germline of *daf-2* mutant produces a synergistic effect on longevity (Chen et al., 2013). The histone H3 lysine 3 trimethylation (H3K3me3) deficiency-induced lifespan extension is also mediated by downregulation of RSKS-1 in the germline, which leads to increased accumulation of mono-unsaturated fatty acids (MUFAs) in the distal intestine tissue (Han et al., 2017). It will be interesting to test whether inhibition of *cyc-2.1* in the germline affects lipid metabolism in the intestine, and if so, whether UPR^{mt} is involved in this process, in future studies.

In conclusion, genome-wide translational state analysis allowed us to identify a series of translational regulation of lifespan-determinant genes in the significantly long-lived *daf-2 rsks-1* mutant. Functional studies revealed that RNA-binding protein GLD-1-mediated translational repression of cytochrome *c* in the germline leads to non-autonomous activation of UPR^{mt} and AMPK in the intestine, which is indispensable for the significantly extended lifespan. In the future, it will be important to understand how the translational regulation is achieved and how the germline signals the distal metabolic tissue upon mitochondrial perturbation at the molecular level.

STAR★METHODS

LEAD CONTACT AND MATERIALS AVAILABILITY

Further information and requests for resources and reagents should be directed to and will be fulfilled by the Lead Contact, Di Chen (chendi@nju.edu.cn; cedauer@gmail.com). The germline-specific RNAi strain DCL569 has been deposited to the Caenorhabditis Genetics Center (https://cgc.umn.edu/strain/DCL569).

EXPERIMENTAL MODEL AND SUBJECT DETAILS

***C. elegans* strains and maintenance—**The following *C. elegans* strains used in this study were obtained from the Caenorhabditis Genome Center: Bristol (N2) strain as the wild-type strain, AA86 *daf-12(rh61rh411) X*, CB1370 *daf-2(e1370) III*, CF1038 *daf-16(mu86) I*, MT2547 *ced-4(n1162) III*, NR222 *rde-1(ne219) V; kzIs9[lin-26p::NLS::GFP + lin-26p::rde-1*(+) + *rol-6]*, SJ4100 *zcIs13[Phsp-6::gfp] V*, SJZ204 *foxSi37[ges-1p::tomm-20::mKate2::HA::tbb-2 3′UTR] I*, TJ1 *cep-1(gk138) I*, TJ1060 *spe-9(hc88) I; rrf-3(b26) II*, VP303 *rde-1(ne219) V; kbIs7[nhx-2p::rde-1*(+) + *rol-6]*, and WM118 *rde-1(ne300) V; neIs9[myo-3p::HA::rde-1*(+) + *rol-6] X*. The following strain used in this study was obtained from the National BioResource Project: *drp-1(tm1108) IV*. The following strains used in this study were generated in D.C. and P.K. labs: DCL4 *rsks-1(ok1255) III*, DCL124 *zcIs13[Phsp-6::gfp] V; aak-2(ok524) X*, DCL178 *cyc-2.1[mkc6(cyc-2.1::3 × flag)] IV*, DCL198 *daf-2(e1370) rsks-1(ok1255) III; cyc-2.1[mkc6(cyc-2.1::3 × flag)] IV*, DCL312 *glp-4(bn2) I*, DCL374 *atfs-1(gk3094) V*, DCL419 *gld-1[mkc28(gld-1::mKate2)] I*, DCL430 *gld-1[mkc28(gld-1::mKate2)] I; daf-2(e1370) rsks-1(ok1255) III*, DCL569 *mkcSi13 [sun-1p::rde-1::sun-1 3′UTR + unc-119(+)] II; rde-1(mkc36) V*, DCL606 *mkcSi13[sun-1p::rde-1::sun-1 3′UTR + unc-119(+)] II; cup-4(ok837) III; rde-1(mkc36) V*, DCL701 *mkcSi51[vha-6p::aak-2::sl2::gfp::unc-54 3′UTR + Cbr-unc-119(+)] II; aak-2(ok542) X*, XA8205 *aak-2(ok524) X*, and XA8222 *daf-2(e1370) rsks-1(ok1255) III*.

Strains in this study were derived from the Bristol N2 background. Nematodes were cultured at 20°C on Nematode Growth Media (NGM) agar plates seeded with *E. coli* OP50 unless otherwise stated (Brenner, 1974).

METHOD DETAILS

Polysomal profiling—Four biological replicates of the wild-type N2 and *daf-2 rsks-1* mutant animals at Day 4 of adulthood were collected for polysomal profiling. Around 10,000 worms per sample were homogenized on ice in 350 μL of lysis buffer (300 mM NaCl, 50 mM Tris-HCl [pH 8.0], 10 mM $MgCl_2$, 1 mM EGTA, 200 μg / ml heparin, 400 U / ml RNAsin, 1.0 mM phenylmethylsulfonyl fluoride, 0.2 mg / ml cyclo-heximide, 1% Triton X-100, 0.1% Sodium Deoxycholate) by 60 strokes with a Teflon homogenizer. Each sample was then supplemented with 700 μL lysis buffer and incubated on ice for 30 minutes before centrifuging at 20,000 g for 15 minutes at 4°C. 0.9 mL of the supernatant was applied to the top of a 10%–50% sucrose gradient in the high salt resolving buffer (140 mM NaCl, 25 mM Tris-HCl [pH 8.0], 10 mM $MgCl_2$) and centrifuged in a Beckman SW41Ti rotor at 38,000 rpm for 90 min at 4°C. Gradients were fractionated using a Teledyne density gradient fractionator with continuous monitoring of absorbance at 252 nm. Translated mRNAs (≥2 ribosomes per mRNA) and total RNAs (from the original lysates) were extracted using the Trizol reagent.

RNA-Seq and bioinformatics analysis—Four biological replicates of translated and total mRNAs from N2 and *daf-2 rsks-1* mutant animals were sent to the University of Minnesota Genomics Center for library construction and pair-ended sequencing with the length of 100 nucleotides, 11.5 million reads per sample on a HiSeq2000 machine

(Illumina). Reads were aligned to the *C. elegans* genome (WS220) using the spliced-junction mapper TopHat2 (Kim et al., 2013). Aligned reads were counted per gene using the python script HTseq (Anders et al., 2015). Differential expression and dataset normalization were performed using the Bioconductor package edgeR (Robinson et al., 2010). Normalization in edgeR was adjusted for RNA composition to ensure that highly expressed genes, which consume a large portion of the RNA pool, did not result in the under-sampling of other genes. Dispersion of the gene counts were estimated tag-wise using the Cox-Reid profile-adjusted likelihood method (Cox and Reid, 1987). Only genes with an average counts per million (CPM) of eight or greater across all conditions were considered for differential expression. Differential expression was calculated pairwise between groups using a general linear model and the resulting *p* values were adjusted for multiple testing sing the Benjamin-Hochberg method (Benjamin and Hochberg, 1995). Changes in post-transcriptional processing were identified by comparing the ratio of polysomal-associated mRNA to total mRNA between the wild-type N2 and *daf-2 rsks-1* mutant animals. This is referred to as Differential Polysome Association Ratio (DPAR), with a positive value indicating an increase in the percentage of a particular species of mRNA associated with polysomes in the *daf-2 rsks-1* mutant.

RNAi by feeding—RNAi experiments were performed by feeding worms *E. coli* strain HT115 (DE3) transformed with either the empty vector L4440 as the control or gene-targeting constructs from the *C. elegans* Ahringer RNAi Collection (Kamath et al., 2001). Overnight bacterial culture in LB supplemented with Ampicillin (100 μg / ml) at 37°C was seeded onto NGM plates containing IPTG (1 mM) and Ampicillin (100 μg / ml) and incubated overnight at room temperature to induce double-stranded RNAs production. Embryos or L1 larvae were placed on RNAi plates and incubated at 20°C until adulthood to score phenotypes.

Lifespan assay—All lifespan assays were performed at 20°C unless otherwise stated. To prevent progeny production during, 20 μg / ml (+)-5-fluoro-deoxyuridine (FUdR) was added onto NGM plates during the reproductive period (Day 1 to 7 of adulthood). The first day of adulthood is Day 1 on survival curves. Animals were scored as alive, dead or lost every other day. Animals that did not respond to gentle touch were scored as dead. Animals that died from causes other than aging, such as sticking to the plate walls, internal hatching or bursting in the vulval region, were scored as lost. Kaplan-Meier survival curves were plotted for each lifespan assay, and statistical analyses (log-rank tests) were performed using the Prism 6 software.

RNAi screen for lifespan regulators—The primary screen was performed using the strain TJ1060 *spe-9(hc88) I; rrf-3(b26) II*, which showed temperature sensitive sterility, enhanced RNAi sensitivity and normal lifespan. Synchronized TJ1060 L1 larvae were transferred onto plates with RNAi against 112 translationally downregulated genes at 25°C until animals reached Day 1 adulthood for survival assays. For the 39 RNAi treatments that caused larval arrest, synchronized TJ1060 L1 larvae were transferred to the control RNAi plates, and day 1 adult animals were then transferred to those 39 RNAi plates for survival assays. Animals were scored as alive, dead or lost every 4-5 days. RNAi treatments that

caused significant lifespan extension ($p < 0.05$, log-rank tests) were selected for two rounds of re-tests in the wild-type N2 background at 20°C. RNAi treatments that caused significant lifespan extension in both re-test groups ($p < 0.05$, log-rank tests) were regarded as positive hits.

Microscopy—Animals were anaesthetized in 1% sodium azide and immediately imaged. The *hsp-6p::*GFP transgenic worms were imaged with a Leica MC165 FC dissecting microscope and a Leica DFC450 C digital camera. GLD-1::mKate2 animals were anaesthetized on 2% agarose pads and imaged with a Zeiss LSM880 confocal microscope. Mitochondria morphology was measured using the transgenic strain *foxSi37[ges-1p::tomm-20::mKate2::HA::tbb-2 3′UTR]*. Day 1 adult animals treated with either the control or *cyc-2.1* RNAi during development were imaged with a Zeiss LSM880 confocal microscope. Filamented and fragmented were defined if majority of the mitochondrial filaments' lengths were longer than 4 μm or shorter than 2 μm, respectively. The rest were defined as intermediate. In all the imaging studies, images within the same figure panel were taken with the same exposure time and adjusted with identical parameters using the Adobe Photoshop or ImageJ.

Western blot and antibodies—For western blots using whole animals, either roughly equal numbers of synchronized Day 1 adult animals were manually transferred into the lysis buffer (150 mM NaCl, 1 mM EDTA, 0.25% SDS, 1.0% NP-40, 50 mM Tris-HCl [pH7.4], Roche complete protease inhibitors and phosSTOP phosphatase inhibitors) supplemented with the 4 x SDS loading buffer and immediately frozen at −80°C, or animals were collected for extracting the total proteins via sonication and quantifying the protein concentrations via Bradford assays. For western blots using dissected tissues, approximately equal amount of biomass in each sample was collected into the same lysis buffer supplemented with the 4 x SDS loading buffer. Samples were boiled for 10 minutes before resolving on precast SDS-PAGE gels (GenScript). Bands of interests were quantified using the ImageJ software and normalized to the intensities of the internal control, which is either α-tubulin or β-actin. Antibodies used in western blots include monoclonal anti-FLAG (Sigma, 1804), monoclonal anti-Tubulin Alpha (Sigma, T6074), anti-Actin (CST, 4967), anti-Phospho-AMPKα (CST, 2535S) and anti-RPS-0, RPS-3, RPL-5 and RPL-25.2 antibodies (Liu et al., 2018).

RT-qPCR—Synchronized Day 1 adult animals were collected, frozen in the Trizol reagent (Takara) and stored at −80°C until total RNA extraction using the Direct-zol RNA mini prep kit (ZYMO Research). The cDNA was synthesized by the reverse transcription system (Takara). The SYBR Green dye (Takara) was used for qPCR reactions carried out in triplicates on a Roche LightCycler 480 real-time PCR machine. Relative gene expression levels were calculated using the $2^{-\Delta\Delta Ct}$ method (Livak and Schmittgen, 2001). RT-qPCR experiments were performed at least three times with consistent results using independent RNA preparations. mRNA levels of *pmp-2* were used for normalization.

Worm tissue micro-dissection—Worms at Day 1 adulthood were transferred into the S buffer (100 mM NaCl and 50 mM potassium phosphate [pH 6.0]) on a glass slide. Heads of animals were cut off near the pharynx using syringe needles to collect the intestine and

gonad. For RT-qPCR assays, 20-30 gonad or intestine tissues were collected in the Trizol reagent for total RNA extraction. For western blots, at least 100 gonad or intestine tissues were collected in the protein extraction buffer.

CRISPR/Cas9 alleles generation—CRISPR engineering to knock-in 3 x FLAG at the C-terminal of CYC-2.1 was performed by microinjection using the homologous recombination approach (Dickinson et al., 2013). The injection mix contained two plasmids that drive expression of two different Cas9-sgRNAs (50 ng/ μl), a selection marker pCFJ90 (P*myo-2*::mCherry::*unc-54*-3′-UTR) (5 ng / μl, Addgene #19327) and a homologous recombination plasmid (50 ng / μl). To generate the sgRNA plasmids, primers were designed with the CRISPR DESIGN tool (https://zlab.bio/guide-design-resources) and inserted into the pDD162 vector (Addgene #47549) using the site-directed mutagenesis kit (TOYOBO SMK-101). To generate the homologous recombination plasmid, the 3 x FLAG coding sequence was first cloned to replace the GFP coding sequence on vector pPD95.77, and two homologous arms (~1,000 bp each) corresponding to the 5′- and 3′-sides of the insertion site, respectively, were then cloned into the same vector. Successful knock-in events were screened by PCR genotyping from independent F1 transgenic animals' progeny that did not carry the co-injection markers, and confirmed by Sanger sequencing.

CRISPR engineering with a self-excising drug selection cassette (SEC) was performed to knock-in the mKate2 fluorescent protein to the C-terminal of GLD-1 (Dickinson et al., 2015). The injection mix contained two plasmids that drive expression of two different Cas9-sgRNAs (50 ng / μl), a selection marker pCFJ90 (P*myo-2*::mCherry::*unc-54*-3′-UTR) (5 ng / μl, Addgene #19327) and a repair template FP-SEC vector (50 ng / μl). To generate the sgRNA plasmids, primers were designed with the CRISPR DESIGN tool (https://zlab.bio/guide-design-resources) and inserted into the pDD162 vector (Addgene #47549) using the site-directed mutagenesis kit (TOYOBO SMK-101). The *ccdB* sequences from the FP-SEC vector pDD287 (Addgene #70685) were replaced with two homologous arms (500-700 bp) to generate the repair template FP-SEC plasmid. Injected animals and their progeny were treated with Hygromycin B (350 μg / ml) to select successful knock-in events. Hygromycin B resistant roller animals were tested by PCR genotyping. The SEC was removed by heat shock and homozygous knock-in alleles were confirmed by PCR and DNA sequencing.

QUANTIFICATION AND STATISTICAL ANALYSIS

Statistical analyses were performed via the Prism 6 (GraphPad) software. Detailed description of tests performed to determine statistical significance is included in figure legends. *, $p < 0.05$; **, $p < 0.01$; ***, $p < 0.001$; ****, $p < 0.0001$; ns, $p > 0.05$.

DATA AND CODE AVAILABILITY

RNA-Seq datasets are available at the NCBI under the accession number GEO: GSE119485.

Supplementary Material

Refer to Web version on PubMed Central for supplementary material.

ACKNOWLEDGMENTS

We thank Drs. Qian Bian, Shiqing Cai, Mengqiu Dong, Arjumand Ghazi, Cole Haynes, Ying Liu, Shohei Mitani, Billy Qi, Ye Tian, Xiaochen Wang, Zhiping Wang, and Steven Zuryn for worm strains, plasmids, antibodies, unpublished results and discussion. Some strains were provided by the CGC, which is funded by NIH Office of Research Infrastructure Programs (P40 OD010440), and some strains were provided by the Japanese National BioResource Project. This work was supported by grants from the National Natural Science Foundation of China (31471379 and 31671527) (to D.C.); by grants from the American Federation for Aging Research, the Larry L. Hillblom Foundation, the Impact Circle Award (Buck), and the NIH (AG053066 and AG045835) (to P.K.); and by grants from the NIH (AG056743), the Morris Scientific Discovery Award, and an Institutional Development Award from the National Institute of General Medical Sciences of the NIH (P20GM103423 and P20GM104318) (to A.N.R.).

REFERENCES

Ahier A, Dai C-Y, Tweedie A, Bezawork-Geleta A, Kirmes I, and Zuryn S (2018). Affinity purification of cell-specific mitochondria from whole animals resolves patterns of genetic mosaicism. Nat. Cell Biol 20, 352–360. [PubMed: 29358705]

Anders S, Pyl PT, and Huber W (2015). HTSeq—a Python framework to work with high-throughput sequencing data. Bioinformatics 31, 166–169. [PubMed: 25260700]

Baruah A, Chang H, Hall M, Yuan J, Gordon S, Johnson E, Shtessel LL, Yee C, Hekimi S, Derry WB, and Lee SS (2014). CEP-1, the *Caenorhabditis elegans* p53 homolog, mediates opposing longevity outcomes in mitochondrial electron transport chain mutants. PLoS Genet. 10, e1004097. [PubMed: 24586177]

Beanan MJ, and Strome S (1992). Characterization of a germ-line proliferation mutation in *C. elegans*. Development 116, 755–766. [PubMed: 1289064]

Benjamin Y, and Hochberg Y (1995). Controlling the False Discovery Rate: a Practical and Powerful Approach to Multiple Testing. J. R. Stat. Soc. Ser. B 57, 289–300.

Berendzen KM, Durieux J, Shao L-W, Tian Y, Kim H-E, Wolff S, Liu Y, and Dillin A (2016). Neuroendocrine Coordination of Mitochondrial Stress Signaling and Proteostasis. Cell 166, 1553–1563.e10. [PubMed: 27610575]

Berman JR, and Kenyon C (2006). Germ-cell loss extends *C. elegans* life span through regulation of DAF-16 by kri-1 and lipophilic-hormone signaling. Cell 124, 1055–1068. [PubMed: 16530050]

Breckenridge DG, Kang B-H, Kokel D, Mitani S, Staehelin LA, and Xue D (2008). *Caenorhabditis elegans* drp-1 and fis-2 regulate distinct cell-death execution pathways downstream of ced-3 and independent of ced-9. Mol. Cell 31, 586–597. [PubMed: 18722182]

Brenner S (1974). The genetics of *Caenorhabditis elegans*. Genetics 77, 71–94. [PubMed: 4366476]

Chen D, Pan KZ, Palter JE, and Kapahi P (2007). Longevity determined by developmental arrest genes in *Caenorhabditis elegans*. Aging Cell 6, 525–533. [PubMed: 17521386]

Chen D, Thomas EL, and Kapahi P (2009). HIF-1 modulates dietary restriction-mediated lifespan extension via IRE-1 in *Caenorhabditis elegans*. PLoS Genet. 5, e1000486. [PubMed: 19461873]

Chen D, Li PW-L, Goldstein BA, Cai W, Thomas EL, Chen F, Hubbard AE, Melov S, and Kapahi P (2013). Germline signaling mediates the synergistically prolonged longevity produced by double mutations in daf-2 and rsks-1 in *C. elegans*. Cell Rep. 5, 1600–1610. [PubMed: 24332851]

Cox DR, and Reid N (1987). Parameter Orthogonality and Approximate Conditional Inference. J. R. Stat. Soc. Ser. B 49, 1–39.

Curran SP, and Ruvkun G (2007). Lifespan regulation by evolutionarily conserved genes essential for viability. PLoS Genet. 3, e56. [PubMed: 17411345]

Depuydt G, Xie F, Petyuk VA, Shanmugam N, Smolders A, Dhondt I, Brewer HM, Camp DG 2nd, Smith RD, and Braeckman BP (2013). Reduced insulin/insulin-like growth factor-1 signaling and dietary restriction inhibit translation but preserve muscle mass in *Caenorhabditis elegans*. Mol. Cell. Proteomics 12, 3624–3639. [PubMed: 24002365]

Dickinson DJ, Ward JD, Reiner DJ, and Goldstein B (2013). Engineering the *Caenorhabditis elegans* genome using Cas9-triggered homologous recombination. Nat. Methods 10, 1028–1034. [PubMed: 23995389]

Dickinson DJ, Pani AM, Heppert JK, Higgins CD, and Goldstein B (2015). Streamlined Genome Engineering with a Self-Excising Drug Selection Cassette. Genetics 200, 1035–1049. [PubMed: 26044593]

Dillin A, Hsu A-L, Arantes-Oliveira N, Lehrer-Graiwer J, Hsin H, Fraser AG, Kamath RS, Ahringer J, and Kenyon C (2002). Rates of behavior and aging specified by mitochondrial function during development. Science 298, 2398–2401. [PubMed: 12471266]

Dong M-Q, Venable JD, Au N, Xu T, Park SK, Cociorva D, Johnson JR, Dillin A, and Yates JR 3rd. (2007). Quantitative mass spectrometry identifies insulin signaling targets in *C. elegans*. Science 317, 660–663. [PubMed: 17673661]

Durieux J, Wolff S, and Dillin A (2011). The cell-non-autonomous nature of electron transport chain-mediated longevity. Cell 144, 79–91. [PubMed: 21215371]

Espelt MV, Estevez AY, Yin X, and Strange K (2005). Oscillatory Ca2+ signaling in the isolated *Caenorhabditis elegans* intestine: role of the inositol 1,4,5-trisphosphate receptor and phospholipases C beta and gamma. J. Gen. Physiol. 126, 379–392. [PubMed: 16186564]

Fontana L, Partridge L, and Longo VD (2010). Extending healthy life span—from yeast to humans. Science 328, 321–326. [PubMed: 20395504]

Han S, Schroeder EA, Silva-García CG, Hebestreit K, Mair WB, and Brunet A (2017). Mono-unsaturated fatty acids link H3K4me3 modifiers to *C. elegans* lifespan. Nature 544, 185–190. [PubMed: 28379943]

Hansen M, Taubert S, Crawford D, Libina N, Lee S-J, and Kenyon C (2007). Lifespan extension by conditions that inhibit translation in *Caenorhabditis elegans*. Aging Cell 6, 95–110. [PubMed: 17266679]

Haynes CM, Petrova K, Benedetti C, Yang Y, and Ron D (2007). ClpP mediates activation of a mitochondrial unfolded protein response in *C. elegans*. Dev. Cell 13, 467–480. [PubMed: 17925224]

Houtkooper RH, Mouchiroud L, Ryu D, Moullan N, Katsyuba E, Knott G, Williams RW, and Auwerx J (2013). Mitonuclear protein imbalance as a conserved longevity mechanism. Nature 497, 451–457. [PubMed: 23698443]

Hsin H, and Kenyon C (1999). Signals from the reproductive system regulate the lifespan of *C. elegans*. Nature 399, 362–366. [PubMed: 10360574]

Hwang AB, Ryu E-A, Artan M, Chang H-W, Kabir MH, Nam H-J, Lee D, Yang J-S, Kim S, Mair WB, et al. (2014). Feedback regulation via AMPK and HIF-1 mediates ROS-dependent longevity in *Caenorhabditis elegans*. Proc. Natl. Acad. Sci. USA 111, E4458–E4467. [PubMed: 25288734]

Kamath RS, Martinez-Campos M, Zipperlen P, Fraser AG, and Ahringer J (2001). Effectiveness of specific RNA-mediated interference through ingested double-stranded RNA in *Caenorhabditis elegans*. Genome Biol 2, RESEARCH0002. PubMed.

Kapahi P, Zid BM, Harper T, Koslover D, Sapin V, and Benzer S (2004). Regulation of lifespan in *Drosophila* by modulation of genes in the TOR signaling pathway. Curr. Biol. 14, 885–890. [PubMed: 15186745]

Kapahi P, Chen D, Rogers AN, Katewa SD, Li PW-L, Thomas EL, and Kockel L (2010). With TOR, less is more: a key role for the conserved nutrient-sensing TOR pathway in aging. Cell Metab. 11, 453–465. [PubMed: 20519118]

Kenyon CJ (2010). The genetics of ageing. Nature 464, 504–512. [PubMed: 20336132]

Kenyon C, Chang J, Gensch E, Rudner A, and Tabtiang R (1993). A *C. elegans* mutant that lives twice as long as wild type. Nature 366, 461–464. [PubMed: 8247153]

Kim Y, and Sun H (2007). Functional genomic approach to identify novel genes involved in the regulation of oxidative stress resistance and animal lifespan. Aging Cell 6, 489–503. [PubMed: 17608836]

Kim D, Pertea G, Trapnell C, Pimentel H, Kelley R, and Salzberg SL (2013). TopHat2: accurate alignment of transcriptomes in the presence of insertions, deletions and gene fusions. Genome Biol. 14, R36. [PubMed: 23618408]

Kimble J, and Crittenden SL (2005). Germline proliferation and its control. WormBook, 1–14.

Kimura KD, Tissenbaum HA, Liu Y, and Ruvkun G (1997). daf-2, an insulin receptor-like gene that regulates longevity and diapause in *Caenorhabditis elegans*. Science 277, 942–946. [PubMed: 9252323]

Korta DZ, Tuck S, and Hubbard EJA (2012). S6K links cell fate, cell cycle and nutrient response in *C. elegans* germline stem/progenitor cells. Development 139, 859–870. [PubMed: 22278922]

Lee SS, Lee RYN, Fraser AG, Kamath RS, Ahringer J, and Ruvkun G (2003). A systematic RNAi screen identifies a critical role for mitochondria in *C. elegans* longevity. Nat. Genet. 33, 40–48. [PubMed: 12447374]

Lin K, Dorman JB, Rodan A, and Kenyon C (1997). daf-16: An HNF-3/ forkhead family member that can function to double the life-span of *Caenorhabditis elegans*. Science 278, 1319–1322. [PubMed: 9360933]

Liu Y, Zou W, Yang P, Wang L, Ma Y, Zhang H, and Wang X (2018). Autophagy-dependent ribosomal RNA degradation is essential for maintaining nucleotide homeostasis during *C. elegans* development. eLife 7, 502.

Livak KJ, and Schmittgen TD (2001). Analysis of relative gene expression data using real-time quantitative PCR and the 2(-Delta Delta C(T)) Method. Methods 25, 402–408. [PubMed: 11846609]

López-Otín C, Blasco MA, Partridge L, Serrano M, and Kroemer G (2013). The hallmarks of aging. Cell 153, 1194–1217. [PubMed: 23746838]

McColl G, Rogers AN, Alavez S, Hubbard AE, Melov S, Link CD, Bush AI, Kapahi P, and Lithgow GJ (2010). Insulin-like signaling determines survival during stress via posttranscriptional mechanisms in C. elegans. Cell Metab. 12, 260–272. [PubMed: 20816092]

McElwee JJ, Schuster E, Blanc E, Thomas JH, and Gems D (2004). Shared transcriptional signature in *Caenorhabditis elegans* Dauer larvae and long-lived daf-2 mutants implicates detoxification system in longevity assurance. J. Biol. Chem. 279, 44533–4543. [PubMed: 15308663]

McQuary PR, Liao C-Y, Chang JT, Kumsta C, She X, Davis A, Chu C-C, Gelino S, Gomez-Amaro RL, Petrascheck M, et al. (2016). *C. elegans* S6K Mutants Require a Creatine-Kinase-like Effector for Lifespan Extension. Cell Rep. 14, 2059–2067. [PubMed: 26923601]

Merkwirth C, Jovaisaite V, Durieux J, Matilainen O, Jordan SD, Quiros PM, Steffen KK, Williams EG, Mouchiroud L, Tronnes SU, et al. (2016). Two Conserved Histone Demethylases Regulate Mitochondrial Stress-Induced Longevity. Cell 165, 1209–1223. [PubMed: 27133168]

Murphy CT, McCarroll SA, Bargmann CI, Fraser A, Kamath RS, Ahringer J, Li H, and Kenyon C (2003). Genes that act downstream of DAF-16 to influence the lifespan of *Caenorhabditis elegans*. Nature 424, 277–283. [PubMed: 12845331]

Nargund AM, Pellegrino MW, Fiorese CJ, Baker BM, and Haynes CM (2012). Mitochondrial import efficiency of ATFS-1 regulates mitochondrial UPR activation. Science 337, 587–590. [PubMed: 22700657]

Nargund AM, Fiorese CJ, Pellegrino MW, Deng P, and Haynes CM (2015). Mitochondrial and nuclear accumulation of the transcription factor ATFS-1 promotes OXPHOS recovery during the UPR(mt). Mol. Cell 58, 123–133. [PubMed: 25773600]

Ogg S, Paradis S, Gottlieb S, Patterson GI, Lee L, Tissenbaum HA, and Ruvkun G (1997). The Fork head transcription factor DAF-16 transduces insulin-like metabolic and longevity signals in *C. elegans*. Nature 389,994–999. [PubMed: 9353126]

Pan KZ, Palter JE, Rogers AN, Olsen A, Chen D, Lithgow GJ, and Kapahi P (2007). Inhibition of mRNA translation extends lifespan in *Caenorhabditis elegans*. Aging Cell 6, 111–119. [PubMed: 17266680]

Patton A, Knuth S, Schaheen B, Dang H, Greenwald I, and Fares H (2005). Endocytosis function of a ligand-gated ion channel homolog in *Caenorhabditis elegans*. Curr. Biol. 15, 1045–1050. [PubMed: 15936276]

Qadota H, Inoue M, Hikita T, Köppen M, Hardin JD, Amano M, Moerman DG, and Kaibuchi K (2007). Establishment of a tissue-specific RNAi system in *C. elegans*. Gene 400, 166–173. [PubMed: 17681718]

Robinson MD, McCarthy DJ, and Smyth GK (2010). edgeR: a Bioconductor package for differential expression analysis of digital gene expression data. Bioinformatics 26, 139–140. [PubMed: 19910308]

Rogers AN, Chen D, McColl G, Czerwieniec G, Felkey K, Gibson BW, Hubbard A, Melov S, Lithgow GJ, and Kapahi P (2011). Life span extension via eIF4G inhibition is mediated by posttranscriptional remodeling of stress response gene expression in *C. elegans*. Cell Metab. 14, 55–66. [PubMed: 21723504]

Selman C, Tullet JMA, Wieser D, Irvine E, Lingard SJ, Choudhury AI, Claret M, Al-Qassab H, Carmignac D, Ramadani F, et al. (2009). Ribosomal protein S6 kinase 1 signaling regulates mammalian life span. Science 326, 140–144. [PubMed: 19797661]

Seo K, Choi E, Lee D, Jeong D-E, Jang SK, and Lee S-J (2013). Heat shock factor 1 mediates the longevity conferred by inhibition of TOR and insulin/IGF-1 signaling pathways in *C. elegans*. Aging Cell 12, 1073–1081. [PubMed: 23879233]

Shao L-W, Niu R, and Liu Y (2016). Neuropeptide signals cell non-autonomous mitochondrial unfolded protein response. Cell Res. 26, 1182–1196. [PubMed: 27767096]

Sheaffer KL, Updike DL, and Mango SE (2008). The Target of Rapamycin pathway antagonizes pha-4/FoxA to control development and aging. Curr. Biol 18, 1355–1364. [PubMed: 18804378]

Shi X, Li J, Zou X, Greggain J, Rødkær SV, Færgeman NJ, Liang B, and Watts JL (2013). Regulation of lipid droplet size and phospholipid composition by stearoyl-CoA desaturase. J. Lipid Res. 54, 2504–2514. [PubMed: 23787165]

Steffen KK, MacKay VL, Kerr EO, Tsuchiya M, Hu D, Fox LA, Dang N, Johnston ED, Oakes JA, Tchao BN, et al. (2008). Yeast life span extension by depletion of 60s ribosomal subunits is mediated by Gcn4. Cell 133, 292–302. [PubMed: 18423200]

Stout GJ, Stigter ECA, Essers PB, Mulder KW, Kolkman A, Snijders DS, van den Broek NJF, Betist MC, Korswagen HC, Macinnes AW, and Brenkman AB (2013). Insulin/IGF-1-mediated longevity is marked by reduced protein metabolism. Mol. Syst. Biol 9, 679. [PubMed: 23820781]

Tian Y, Garcia G, Bian Q, Steffen KK, Joe L, Wolff S, Meyer BJ, and Dillin A (2016). Mitochondrial Stress Induces Chromatin Reorganization to Promote Longevity and UPR(mt). Cell 165, 1197–1208. [PubMed: 27133166]

Williams GC (1957). Pleiotropy, Natural Selection, and the Evolution of Senescence. Evolution 11, 398–411.

Yee C, Yang W, and Hekimi S (2014). The intrinsic apoptosis pathway mediates the pro-longevity response to mitochondrial ROS in *C. elegans*. Cell 157, 897–909. [PubMed: 24813612]

Zhang Q, Wu X, Chen P, Liu L, Xin N, Tian Y, and Dillin A (2018). The Mitochondrial Unfolded Protein Response Is Mediated Cell-Non-autonomously by Retromer-Dependent Wnt Signaling. Cell 174, 870–883.e17. [PubMed: 30057120]

Zid BM, Rogers AN, Katewa SD, Vargas MA, Kolipinski MC, Lu TA, Benzer S, and Kapahi P (2009). 4E-BP extends lifespan upon dietary restriction by enhancing mitochondrial activity in *Drosophila*. Cell 139, 149–160. [PubMed: 19804760]

Zou L, Wu D, Zang X, Wang Z, Wu Z, and Chen D (2019). Construction of a germline-specific RNAi tool in *C. elegans*. Sci. Rep. 9, 2354. [PubMed: 30787374]

Highlights

- Longevity of *daf-2 rsks-1* is mediated by translational repression of *cyc-2.1*
- Germline inhibition of *cyc-2.1* activates intestinal UPR^{mt} and AMPK to extend lifespan
- Increased GLD-1 represses germline *cyc-2.1* translation in the *daf-2 rsks-1* mutant
- Translational regulation of *cyc-2.1* and UPR^{mt} contribute to longevity of *daf-2 rsks-1*

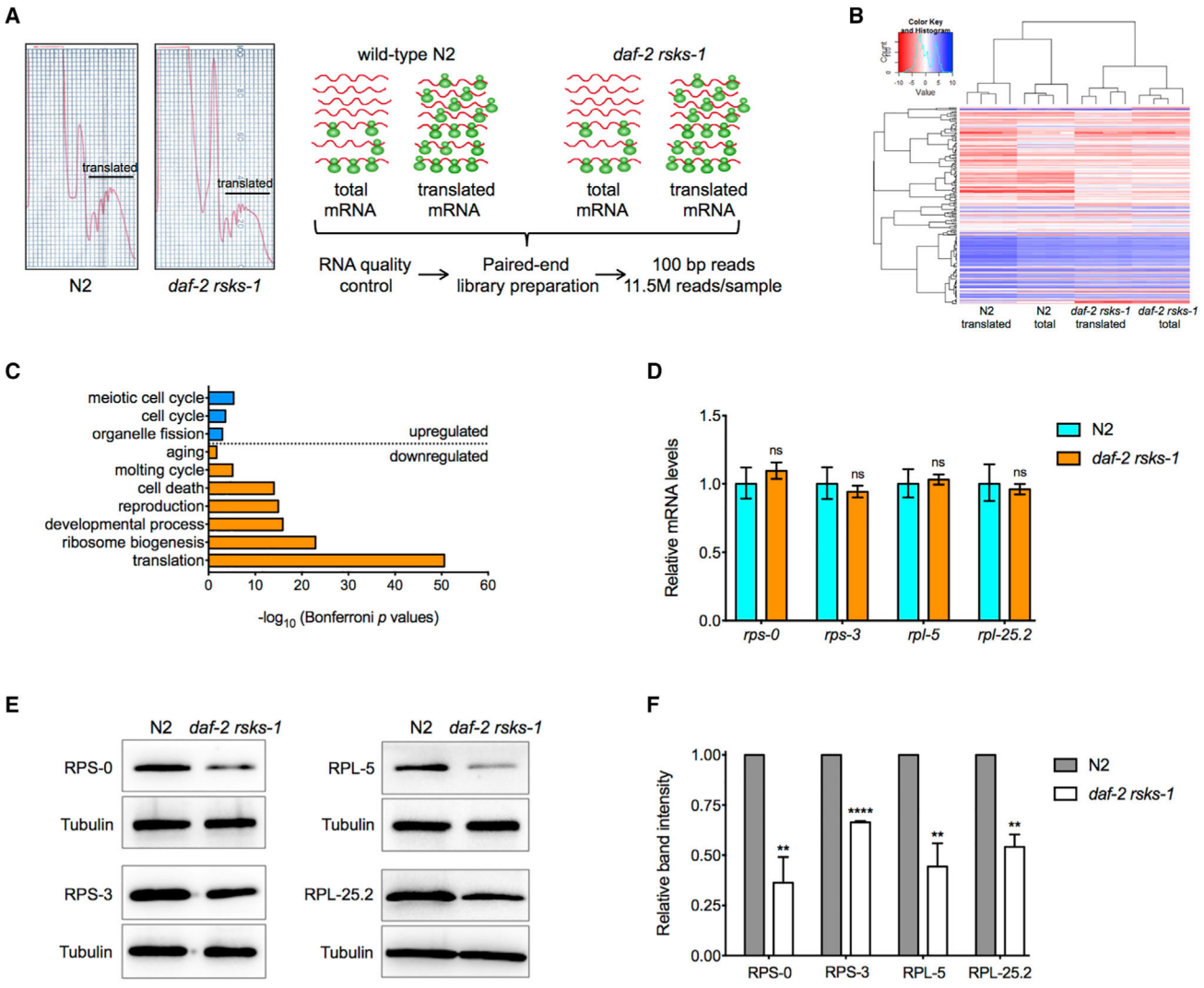

Figure 1. Identification of Genes that Are Translationally Regulated in the *daf-2 rsks-1* Mutant

(A) Experimental design of the genome-wide translational state analysis. On the left are representative polysome profiles of wild-type N2 and the *daf-2 rsks-1* double mutant. The total and translated mRNA fractions were used for the genome-wide transcriptional and translational state analysis, as depicted by the workflow on the right.

(B) Cluster of genes differentially expressed in the *daf-2 rsks-1* mutant compared with N2.

(C) Top Gene Ontology (GO) terms for genes differentially expressed at the translational level in the *daf-2 rsks-1* mutant.

(D) qRT-PCR of *rps-0, rps-3, rpl-5,* and *rpl-25.2* mRNA levels (median with range) in N2 and the *daf-2 rsks-1* mutant based on three biological replicates (not significant [ns], $p > 0.05$, two-tailed t tests).

(E and F) Immunoblots (E) and quantification (F) of RPS-0, RPS-3, RPL-5, RPL-25.2, and tubulin protein levels in N2 and the *daf-2 rsks-1* mutant. The ratio of band intensity of ribosomal proteins to tubulin was normalized to N2. Data are represented as mean ± SEM based on three biological replicates (****$p < 0.0001$, **$p < 0.01$, two-tailed t tests).

See also Table S1.

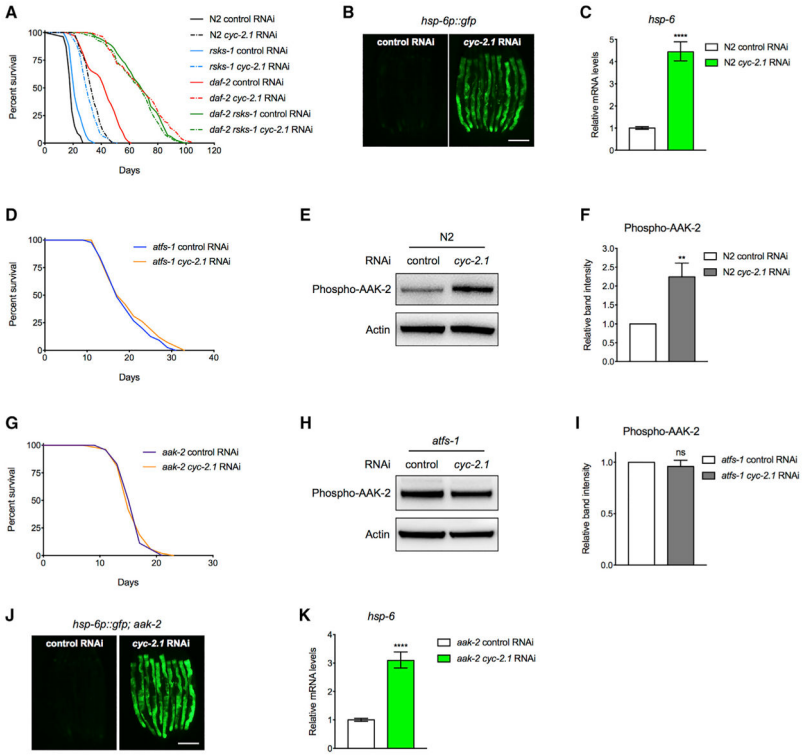

Figure 2. Knockdown of *cyc-2.1* Significantly Extends Lifespan by Activating UPR^{mt} and AMPK

(A) Survival curves of the wild-type N2, *rsks-1, daf-2,* and *daf-2 rsks-1* mutant animals treated with control or *cyc-2.1* RNAi.

(B) Representative photographs of *hsp-6p::gfp* expression in animals treated with control or *cyc-2.1* RNAi. Scale bar, 200 μm.

(C) qRT-PCR of *hsp-6* (median with range) using RNAs extracted from dissected intestinal tissues of N2 treated with control or *cyc-2.1* RNAi based on three biological replicates (****p < 0.0001, two-tailed t test).

(D) Survival curves of the *atfs-1* deletion mutant treated with control or *cyc-2.1* RNAi (p = 0.2355, log-rank test).

(E and F) Immunoblots (E) and quantification (F) of phospho-AAK-2 (AMPKα) and actin in N2 animalstreated with control or *cyc-2.1* RNAi. Ratio of band intensity of phospho-AAK-2 to actin was normalized to the control RNAi-treated animals. Data are represented as mean ± SEM based on eight biological replicates (**p = 0.0041, two-tailed t test).

(G) Survival curves of the *aak-2* deletion mutant treated with control or *cyc-2.1* RNAi (p = 0.9647, log-rank test).

(H and I) Immunoblots (H) and quantification (I) of phospho-AAK-2 and actin in the *atfs-1* deletion mutant treated with control or *cyc-2.1* RNAi. Data are represented as mean ± SEM based on four biological replicates (ns, p = 0.5239, two-tailed t test).

(J) Representative photographs of *hsp-6p::gfp* expression in *aak-2* deletion mutant animals treated with control or *cyc-2.1* RNAi. Scale bar, 200 μm.

(K) qRT-PCR of *hsp-6* (median with range)using RNAs extracted from dissected intestinal tissues of the *aak-2* mutant treated with control or *cyc-2.1* RNAi based on three biological replicates (****p < 0.0001, two-tailed t test) .

See also Table S3.

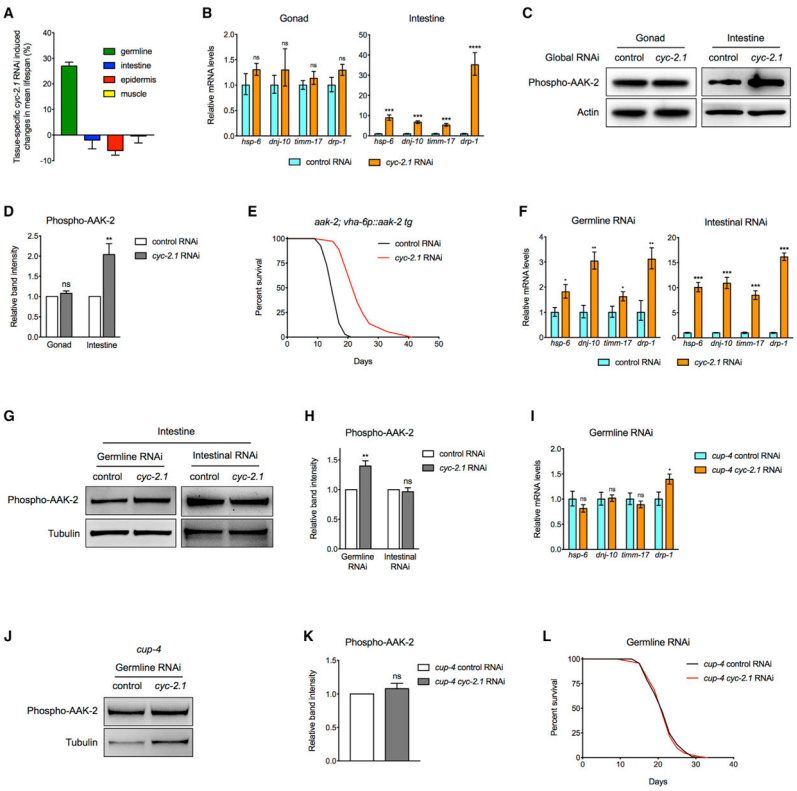

Figure 3. Inhibition of *cyc-2.1* in the Germline Extends Lifespan by Cell-Non-autonomous Activation of UPR^{mt} and AMPK in the Intestine

(A) Tissue-specific *cyc-2.1* RNAi-induced changes in the mean lifespan relative to the control RNAi treatments. Data are represented as mean ± SEM based on three biological replicates.

(B) qRT-PCR of UPR^{mt} markers *hsp-6, dnj-10, timm-17,* and *drp-1* (median with range) using RNAs extracted from dissected gonadal and intestinal tissues of N2 treated with global control or *cyc-2.1* RNAi based on three biological replicates (ns, ***$p < 0.001$, $p > 0.05$, two-tailed t tests).

(C and D) Immunoblots (C) and quantification (D) of phospho-AAK-2 and actin using proteins extracted from dissected gonadal and intestinal tissues of N2 treated with global control or *cyc-2.1* RNAi. Data are represented as mean ± SEM based on three biological replicates (ns, **$p < 0.01$, $p = 0.2436$, two-tailed t tests).

(E) Survival curves of the *aak-2* mutant carrying an *aak-2* transgene driven by the intestine-specific *vha-6* promoter treated with the control or *cyc-2.1* RNAi ($p < 0.0001$, log-rank test).

(F) qRT-PCR of UPR^{mt} markers (median with range) using RNAs extracted from dissected intestinal tissues of animals treated with germline- or intestine-specific control versus *cyc-2.1* RNAi based on three biological replicates (***$p < 0.001$, **$p < 0.01$, *$p < 0.05$, two-tailed t tests).

(G and H) Immunoblots (G) and quantification (H) of phospho-AAK-2 and tubulin using proteins extracted from dissected intestinal tissues of animals treated with germline- or intestine-specific control versus *cyc-2.1* RNAi. Data are represented as mean ± SEM based on three biological replicates(ns, **$p < 0.001$, $p = 0.6141$, two-tailed t tests).

(I) qRT-PCR of UPR^{mt} markers (median with range) using RNAs extracted from dissected intestinal tissues of the *cup-4* mutant treated with germline-specific control or *cyc-2.1* RNAi based on three biological replicates (ns, *$p < 0.05$, $p > 0.05$, two-tailed t tests).
(J and K) Immunoblots (J) and quantification (K) of phospho-AAK-2 and tubulin using proteins extracted from dissected intestinal tissues of the *cup-4* mutant treated with germline-specific control or *cyc-2.1* RNAi. Data are represented as mean ± SEM based on three biological replicates (ns, $p = 0.3957$, two-tailed t tests).
(L) Survival curves of the *cup-4* mutant treated with germline-specific control or *cyc-2.1* RNAi ($p = 0.8629$, log-rank test).
See also Figure S3 and Table S3.

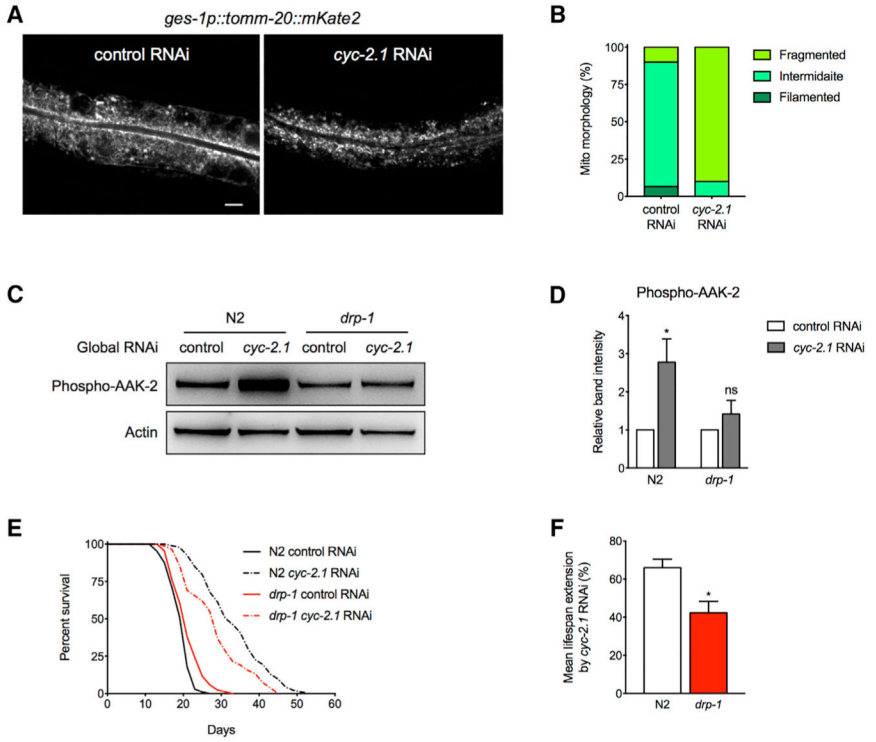

Figure 4. *cyc-2.1* Knockdown-Induced Mitochondria Fragmentation Plays an Important Role in AMPK Activation and Lifespan Extension

(A and B) Representative photographs (A) and quantification (B) of intestinal mitochondrial morphology in animals treated with control or *cyc-2.1* RNAi ($p < 0.0001$, χ^2 test). Scale bar, 10 μm.

(C and D) Immunoblots (C) and quantification (D) of phospho-AAK-2 and actin in N2 and *drp-1* mutant animals treated with control or *cyc-2.1* RNAi. Data are represented as mean ± SEM based on three biological replicates (ns, $^*p < 0.05$, $p = 0.3103$, two-tailed t tests).

(E) Survival curves of N2 and the *drp-1* mutant treated with control or *cyc-2.1* RNAi.

(F) *cyc-2.1* RNAi-induced changes in mean lifespan relative to the control RNAi treatments in N2 and *drp-1* mutant backgrounds. Data are represented as mean ± SEM based on three biological replicates ($^*p < 0.05$, two-tailed t test).

See also Table S3.

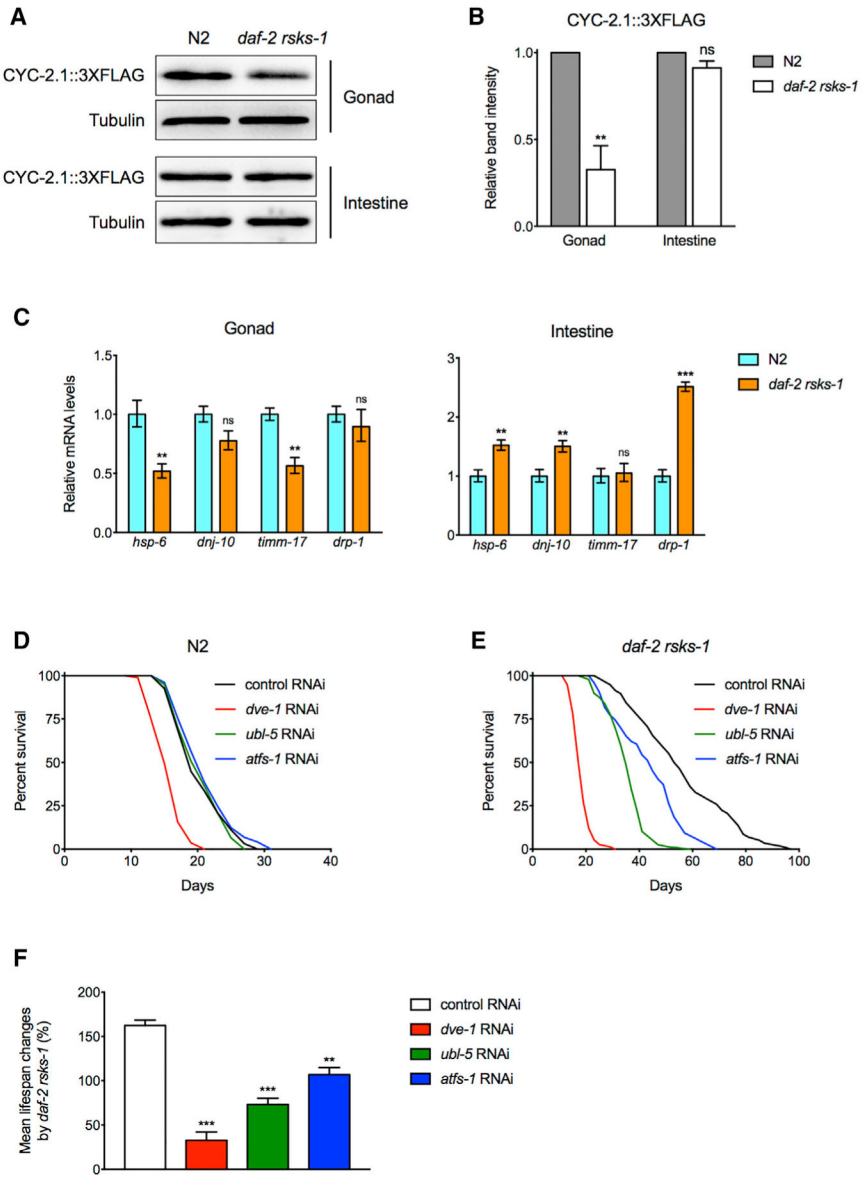

Figure 5. Translational Repression of CYC-2.1 in the Germline and Non-autonomous Activation of UPR^{mt} in the Intestine Play an Important Role in Regulating the Synergistic Lifespan Extension by *daf-2 rsks-1*

(A and B) Immunoblots (A) and quantification (B) of CYC-2.1::3x FLAG and tubulin using proteins extracted from dissected gonadal and intestinal tissues of N2 and *daf-2 rsks-1* mutant animals. Data are represented as mean ± SEM based on three biological replicates (ns, **$p < 0.01$, $p = 0.0880$, two-tailed t tests).

(C) qRT-PCR of UPR^{mt} markers (median with range) using RNAs extracted from dissected gonadal and intestinal tissues of N2 and *daf-2 rsks-1* mutant animals based on three biological replicates (ns, ***$p < 0.001$, **$p < 0.01$, $p > 0.05$, two-tailed t tests).

(D and E) Survival curves of N2 (D) and the *daf-2 rsks-1* mutant (E) treated with the control, *dve-1, ubl-5,* or *atfs-1* RNAi.

(F) The *daf-2 rsks-1* double mutations induced changes in mean lifespan upon control, *dve-1, ubl-5,* or *atfs-1* RNAi treatment. Data are represented as mean ± SEM based on three biological replicates (***p < 0.001, **p < 0.01, two-tailed t tests).
See also Table S3.

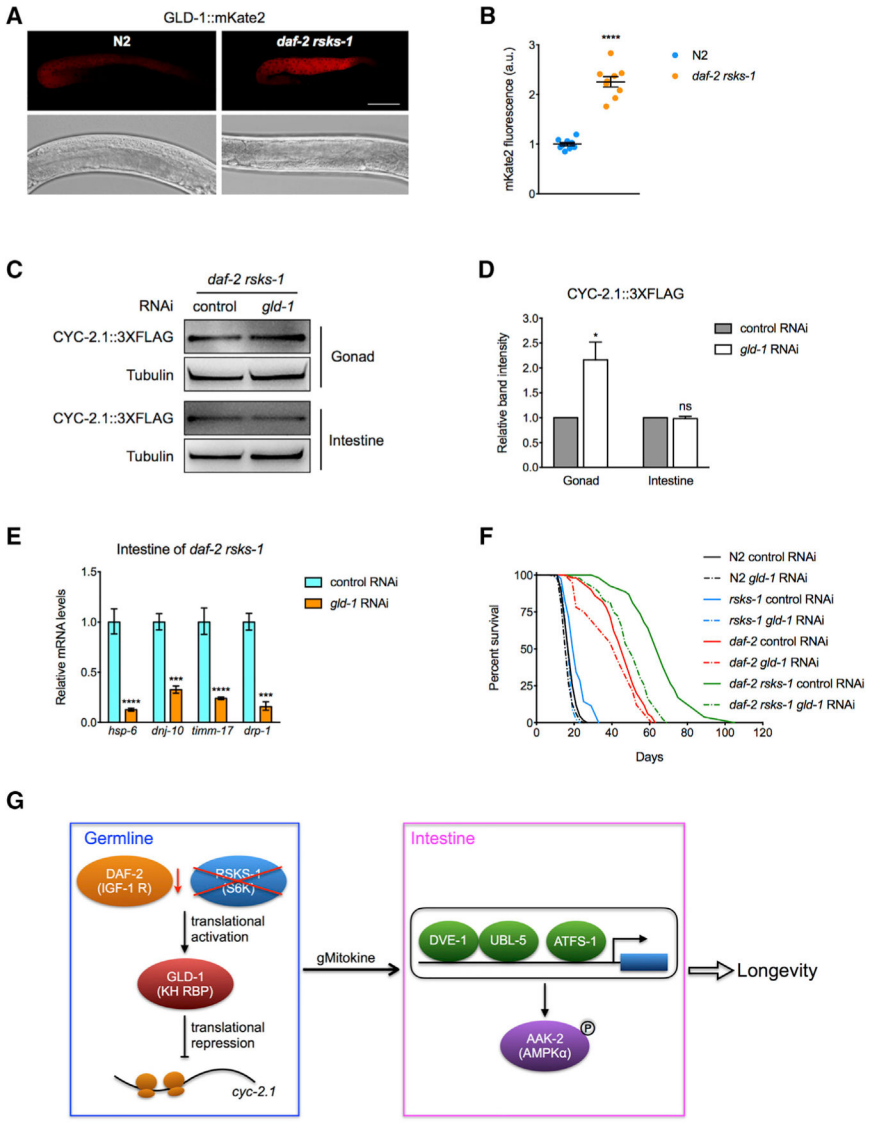

Figure 6. Translational Repression of *cyc-2.1* by GLD-1 Contributes to the UPR^{mt} Activation and Lifespan Extension in the *daf-2 rsks-1* Mutant

(A and B) Representative photographs (A) and quantification (B) of GLD-1::mKate2 expression in the germline of N2 and *daf-2 rsks-1* mutant animals. Data are represented as mean ± SEM (****$p < 0.0001$, two-tailed t test). Scale bar, 50 μm.

(C and D) Immunoblots (C) and quantification (D) of CYC-2.1::3x FLAG and tubulin using proteins extracted from dissected gonadal and intestinal tissues of N2 and *daf-2 rsks-1* mutant animals. Data are represented as mean ± SEM based on three biological replicates (ns, *$p < 0.05$, $p = 0.7063$, two-tailed t tests).

(E) qRT-PCR of UPR^{mt} markers (median with range) using RNAs extracted from dissected intestinal tissues of the *daf-2 rsks-1* mutant treated with the control versus *gld-1* RNAi based on three biological replicates (****$p < 0.0001$, ***$p < 0.001$, two-tailed t tests).

(F) Survival curves of the wild-type N2, *rsks-1, daf-2,* and *daf-2 rsks-1* mutant animals treated with control or *gld-1* RNAi.

(G) Model depicting the translational repression of CYC-2.1 by GLD-1 in the germline non-autonomously activates UPR^{mt} and AMPK in the intestine via germline-produced mitokine (gMitokine) signaling, which leads to significant lifespan extension in the *daf-2 rsks-1* mutant.

See also Table S3.

KEY RESOURCES TABLE

REAGENT or RESOURCE	SOURCE	IDENTIFIER
Antibodies		
β-Actin Antibody	Cell Signaling Technology	RRID: AB_330288; Cat# 4967
Phospho-AMPKα (Thr172) (40H9) Rabbit mAb	Cell Signaling Technology	RRID: AB_331250; Cat# 2535S
Monoclonal Anti-α-Tubulin antibody	Sigma-Aldrich	RRID: AB_477582; Cat# T6074
Monoclonal Anti-FLAG antibody	Sigma-Aldrich	RRID: AB_262044; Cat# F1804
Anti-RPS-0 antibody	Liu et al., 2018	N/A
Anti-RPS-3 antibody	Liu et al., 2018	N/A
Anti-RPL-5 antibody	Liu et al., 2018	N/A
Anti-RPL-25.2 antibody	Liu et al., 2018	N/A
Goat Anti-Rabbit IgG (H+L) HRP	Bioworld	RRID: AB_2773728; Cat# BS13278
Goat Anti-Mouse IgG (H+L) HRP	Bioworld	RRID: AB_2773727; Cat# BS12478
Bacterial and Virus Strains		
E. coli: Strain OP50	Caenorhabditis Genetics Center	N/A
E. coli: Strain HT115	Caenorhabditis Genetics Center	N/A
C. elegans RNAi Library (Ahringer)	Source BioScience	3318_Cel_RNAi_complete
Chemicals, Peptides, and Recombinant Proteins		
Taq DNA Polymerase	ABM	Cat# G008
T4 ligase	ABM	Cat# EL0011
Ligation-Free Cloning Kit	ABM	Cat# E002
Ampicillin	BBI	Cat# AB0028
Peptone	BD	Cat# 211677
Agar	BD	Cat# 214010
Tryptone	BD	Cat# 211705
Yeast Extract	BD	Cat# 212750
Agar	BD	Cat# 214010
Biodlight Western Chemiluminescent HRP substrate	Bioworld	Cat# BLH02S050
Proteinase K	Fermentas	Cat# EO0491
FastAP Thermosensitive Alkaline Phosphatase	Fermentas	Cat# EF0654
ExpressPlus PAGE Gel	GenScript	Cat# M42015C
Tris-MOPS-SDS Running Buffer	GenScript	Cat# M00138
PVDF	Immobilon	Cat# IPVH00010
cOmplete, EDTA-free Protease Inhibitor Cocktail	Roche	Cat# 4693132001
PhosSTOP	Roche	Cat# 4906845001
dNTP	Sangon	Cat# D0056
Ethidium bromide	Sangon	Cat# EX328
Sodium chloride	Sangon	Cat# A100241
Sodium dodecyl sulfate (SDS)	Sangon	Cat# S0227
EDTA	Sangon	Cat# EB0185
Tris (Base)	Sangon	Cat# TT1492

REAGENT or RESOURCE	SOURCE	IDENTIFIER
Potassium chloride	Sangon	Cat# A501212-0500
Magnesium sulfate anhydrous ($MgSO_4$)	Sangon	Cat# A601988-0250
Calcium chloride ($CaCl_2$)	Sangon	Cat# 10035-04-8
Isopropyl-b-D-thiogalactoside (IPTG)	Sangon	Cat# IB0168
Potassium phosphate dibasic (K_2HPO_4)	Sangon	Cat# PT1212
Potassium phosphate monobasic (KH_2PO_4)	Sangon	Cat# A600445
Tetracycline	Sangon	Cat# G0167
Protein ladder	Sangon	Cat# AB0072
Glycine	Sangon	Cat# T0761
APS, Ammonium persulfate	Sangon	Cat# M0004
TEMED	Sangon	Cat# SN319
β-Mercaptoethanol	Sangon	Cat# NB0669
30% Acryl/Bis Solution	Sangon	Cat# SN319
NON-Fat Powdered Milk	Sangon	Cat# NB0669
Hygromycin B	Sangon	Cat# A600230-0001
Triton X-100	Sangon	Cat# A110694
NP-40	Sigma-Aldrich	Cat# 74388
Tween-20	Sigma-Aldrich	Cat# P9416
Cholesterol	Sigma-Aldrich	Cat# C3045
FUDR	Sigma-Aldrich	Cat# F6627
PrimeSTAR Max DNA Polymerase (HD)	TAKARA	Cat# R045A
Trizol	TAKARA	Cat# 9108
Hind III	TAKARA	Cat# 1060A
BamH I	TAKARA	Cat# 1010A
Spe I	TAKARA	Cat# 1086A
KpnI	TAKARA	Cat# 1068A
PstI	TAKARA	Cat# 1073A
Dpn I	TAKARA	Cat# 1235A
SYBR Premix Ex TaqTM II	TAKARA	Cat# RR820A
PageRuler Prestained protein ladder	Thermo Scientific	Cat# 26616
NuPAGE LDS Sample Buffer(4X)	Thermo Fisher	Cat# NP0007
Trans 2k plus DNA marker	Transgene	Cat# BM111
Agarose	Vivantis	Cat# PC0701
Critical Commercial Assays		
PCR clean-up Kit	Axygen	Cat# AP-PCR
Plasmid mini prep	Axygen	Cat# AP-MN-P
Pure link Quick Plasmid mini prep kit	Invitrogen	Cat# K210011
Pierce BCA Protein Assay Kit	Pierce	Cat# 23227
PrimeScript RT reagent Kit with gDNA Eraser	TAKARA	Cat# RR047A
KOD-Plus-Mutagenesis kit	TOYOBO	Cat# SMK-101
Direct-zol RNA mini prep	Zymo Research	Cat# R2052
Deposited Data		

REAGENT or RESOURCE	SOURCE	IDENTIFIER
RNA-Sequencing data of translated mRNA and total mRNA in N2	This Study	GEO: GSE119485
RNA-Sequencing data of translated mRNA and total mRNA in *daf-2 rsks-1*	This Study	GEO: GSE119485
Experimental Models: Organisms/Strains		
C. elegans: strain N2: wild isolate	Caenorhabditis Genetics Center	N/A
C. elegans: strain AA86 *daf-12(rh61rh411) X*	Caenorhabditis Genetics Center	N/A
C. elegans: strain CB1370 *daf-2(e1370) III*	Caenorhabditis Genetics Center	N/A
C. elegans: strain CF1038 *daf-16(mu86) I*	Caenorhabditis Genetics Center	N/A
C. elegans: strain MT2547 *ced-4(n1162) III*	Caenorhabditis Genetics Center	N/A
C. elegans: strain NR222 *rde-1(ne219) V; kzIs9[lin-26p::NLS::GFP + lin-26p::rde-1*(+) + *rol-6]*	Caenorhabditis Genetics Center	N/A
C. elegans: strain SJ4100 *zcIs13[Phsp-6::gfp] V*	Caenorhabditis Genetics Center	N/A
C. elegans: strain SJZ204 *foxSi37[ges-1p::tomm-20:: mKate2::HA::tbb-2 3′UTR] I*	Caenorhabditis Genetics Center	N/A
C. elegans: strain TJ1 *cep-1(gk138) I*	Caenorhabditis Genetics Center	N/A
C. elegans: strain TJ1060 *spe-9(hc88) I; rrf-3(b26) II*	Caenorhabditis Genetics Center	N/A
C. elegans: strain WM118 *rde-1(ne300) V; neIs9[myo-3p::HA::rde-1*(+) + *rol-6] X*	Caenorhabditis Genetics Center	N/A
C. elegans: strain VP303 *rde-1(ne219) V; kbIs7[nhx-2p::rde-1*(+) + *rol-6]*	Caenorhabditis Genetics Center	N/A
C. elegans: strain CU6372 *drp-1(tm1108) IV*	Japanese National BioResource Project	N/A
C. elegans: strain DCL4 *rsks-1(ok1255) III*	This paper	N/A
C. elegans: strain DCL124 *zcIs13[Phsp-6::gfp] V; aak-2(ok524) X*	This paper	N/A
C. elegans: strain DCL178 *cyc-2.1[mkc6(cyc-2.1::3Xflag)] IV*	This paper	N/A
C. elegans: strain DCL198 *daf-2(e1370) rsks-1(ok1255) III; cyc-2.1[mkc6(cyc-2.1::3Xflag)] IV*	This paper	N/A
C. elegans: strain DCL312 *glp-4(bn2) I*	This paper	N/A
C. elegans: strain DCL374 *atfs-1(gk3094) V*	This paper	N/A
C. elegans: strain DCL419 *gld-1[mkc28(gld-1::mKate2)] I*	This paper	N/A
C. elegans: strain DCL430 *gld-1[mkc28(gld-1::mKate2)] I; daf-2(e1370) rsks-1(ok1255) III*	This paper	N/A
C. elegans: strain DCL569 *mkcSi13[sun-1p::rde-1::sun-13′UTR + unc-119(+)] II; rde-1(mkc36) V*	This paper	N/A
C. elegans: strain DCL606 *mkcSi13[sun-1p::rde-1::sun-1 3′UTR + unc-119(+)] II; cup-4(ok837) III; rde-1(mkc36) V*	This paper	N/A
C. elegans: strain DCL701 *mkcSi51[vha-6p::aak-2::sl2:: gfp::unc-54 3′ UTR + Cbr-unc-119(+)] II; aak-2(ok542) X*	This paper	N/A
C. elegans: strain XA8205 *aak-2(ok524)* X	This paper	N/A
C. elegans: strain XA8222 *daf-2(e1370) rsks-1(ok1255)* III	This paper	N/A
Oligonucleotides		
For primers used for RT-qPCR, RNAi constructs and gene editing via CRISPR/Cas9, see Table S4	This paper	N/A

REAGENT or RESOURCE	SOURCE	IDENTIFIER
Software and Algorithms		
TopHat2	Kim et al., 2013	http://ccb.jhu.edu/software/tophat
HTseq	Anders et al., 2015	http://htseq.readthedocs.io/en/release_0.10.0/
edgeR	Robinson et al., 2010	https://www.bioconductor.org/
Cox-Reid profile-adjusted likelihood method	Cox and Reid, 1987	N/A
Benjamin-Hochberg method	Benjamin and Hochberg, 1995	N/A
GraphPad Prism version 6	GraphPad Software	https://www.graphpad.com/
Snapgene Viewer	Snapgene	http://www.snapgene.com/